The Canadian Mineralogist
Vol. 43, pp. 157-182 (2005)

DIFFUSION-CONTROLLED SYNKINEMATIC GROWTH OF GARNET FROM A HETEROGENEOUS PRECURSOR AT PASSO DEL SOLE, SWITZERLAND

CHARNA E. METH AND WILLIAM D. CARLSON§

Department of Geological Sciences, University of Texas at Austin, Austin, Texas 78712, U.S.A.

ABSTRACT

Synkinematic porphyroblasts of garnet from Passo del Sole, Switzerland, display textural and chemical characteristics that record crystallization mechanisms governed by intergranular diffusion and influenced by compositional heterogeneity. Quantitative textural analysis yields evidence for size–isolation correlations, reflecting diffusional suppression of growth due to competition for nutrients among neighboring crystals. Compositional zoning, including extraordinary oscillatory zoning of Ca, reveals a previously undocumented relationship: a direct proportionality between the radii of crystals and their rates of radial growth. That relationship arises in diffusion-controlled growth from a heterogeneous precursor: slow intergranular diffusion preserves local heterogeneities in the distribution of nutrients, causing crystals to grow at a rate dependent upon the local supply of nutrients; thus faster-growing crystals are larger at all stages of the process. These results therefore provide no support for the hypothesis that deformation during metamorphism eliminates diffusional controls on porphyroblast growth by accelerating transportation of nutrients. Variable extents of chemical equilibration during growth are reflected in variable degrees of uniformity in chemical zoning among crystals of garnet. In concert with prior findings, Fe and Mg appear to have equilibrated rock-wide throughout the crystallization interval, whereas low Mn concentrations in garnet cores, for crystals in textural settings that would restrict diffusional supply, indicate disequilibrium for Mn during early, low-temperature growth. In contrast with prior findings, intricate yet identical patterns of oscillatory Ca zoning in all crystals indicate equilibration rock-wide for Ca during most, if not all, of the crystallization interval.

Keywords: intergranular diffusion, crystal growth, crystallization kinetics, disequilibrium, garnet, Swiss Alps.

SOMMAIRE

Nous décrivons des porphyroblastes syncinématiques de grenat provenant de Passo del Sole, en Suisse, qui font preuve de caractéristiques texturales et chimiques typiques de mécanismes de cristallisation régis par une diffusion intergranulaire et influencés par une hétérogénéité compositionnelle. Une analyse texturale quantitative mène à une indication de corrélations entre dimension et degré d'isolation, qui témoignent de la suppression de la diffusion au cours de la croissance, due à la compétition pour les éléments nutritifs requis parmi les cristaux voisins. Une zonation en composition, en particulier une zonation oscillatoire exceptionelle en Ca, révèle une relation non documentée auparavant: il y a une proportionalité directe entre le rayon des cristaux et leur taux de croissance radiale. Cette relation découle d'une croissance régie par la diffusion à partir d'un précurseur hétérogène; une diffusion intergranulaire lente conserve les hétérogénéités locales dans la distribution des éléments nutritifs requis pour la croissance, ce qui a causé une croissance des cristaux à un taux dépendant de la disponibilité locale de ces éléments; les cristaux qui ont cru plus rapidement sont plus gros à tous les stades du processus. Ces résultats ne concordent donc pas avec l'hypothèse voulant que la déformation au cours du métamorphisme puisse éliminer les influences de la diffusion sur la croissance des porphyroblastes par tranfert accéléré des éléments nutritifs. Des taux variables de ré-équilibrage chimique au cours de la croissance mènent à des degrés variables d'uniformité en zonation chimique parmi les cristaux de grenat. Tout comme dans la documentation précédente, le Fe et le Mg semblent avoir pu s'équilibrer à l'échelle de la roche tout au long de l'intervalle de cristallisation, tandis que le manganèse, en faibles quantités dans le coeur des cristaux aptes à subir des restrictions en disponibilité de cet élément, indique un déséquilibre aux stades précoces de la croissance, à faible température. En revanche, et contrairement à ce que l'on pourrait s'attendre suite aux études précédentes, des tracés complexes mais identiques en zonation oscillatoire en Ca font penser que l'équilibrage était atteint à l'échelle de la roche pour le Ca pour la plupart, sinon toute, la durée de la cristallisation du grenat.

(Traduit par la Rédaction)

Mots-clés: diffusion intergranulaire, croissance cristalline, cinétique de cristallisation, déséquilibre, grenat, Alpes Suisses.

§ *E-mail address*: wcarlson@mail.utexas.edu

Introduction

Dugald Carmichael's insightful description of the mechanism of prograde metamorphic reactions in quartz-bearing pelitic rocks (Carmichael 1969) long ago alerted petrologists to the importance of intergranular diffusion during metamorphic crystallization, and yet we still strive to assess its textural and chemical impacts. Carmichael's now-classic analysis was the first treatment to demonstrate clearly that reaction mechanisms can be determined by different relative rates of intergranular diffusion for different elements. His study emphasized the dominant control provided by the sluggish transport of aluminous species: because diffusion of Al is very slow, small subdomains exist in metamorphic rocks within which Al is essentially conserved; during reaction, these subdomains communicate chemically across larger distances by the transport of more rapidly diffusing species.

Subsequent work has expanded this fundamental concept in many ways. Most significant have been efforts to elaborate our understanding of the controls that intergranular diffusion can exert on metamorphic textures and microstructures (*e.g.*, Joesten 1977, Foster 1986, Carlson 1989, Johnson & Carlson 1990, Carlson & Denison 1992, Denison & Carlson 1997, Spear & Daniel 2001), and efforts to assess the negative impact that differences in rates of intergranular diffusion for different elements can have on the establishment of chemical equilibrium during metamorphism (*e.g.*, Chernoff & Carlson 1997, 1999, Yang & Rivers 2001, Carlson 2002).

The present study contributes to both of these efforts. Prior investigations of mechanisms of metamorphic reaction have largely, though not exclusively, focused intentionally on simple modes of crystallization: growth from homogeneous precursors in the absence of deviatoric stresses. In this work, we add new levels of complexity by considering synkinematic growth of porphyroblasts from a heterogeneous precursor. Crystallization under such conditions is common and conceivably could obey fundamentally different kinetics. Nucleation-and-growth kinetics might be strongly modified by heterogeneities in nucleation-site density and in the distribution of nutrients required for crystal growth, yielding significant textural variations that affect mechanisms of chemical exchange among reactants and products. Deformation might enhance diffusion by dynamically altering the network of grain-edge pathways, or it might allow introduction of fluids as a means of advective transport that could eliminate intergranular diffusion as a rate-controlling factor; either effect might remove the potential for partial chemical disequilibrium that diffusion-controlled processes impose on crystallization. These possibilities are addressed here by combining quantitative textural analysis with detailed examination of chemical zoning in synkinematic porphyroblasts of garnet in a heterogeneous pelitic gneiss from Passo del Sole in the central Swiss Alps.

Background: Crystallization Mechanisms and Kinetics

The mechanisms and kinetics of processes required for the nucleation and growth of porphyroblasts find direct expression in the textural and chemical features of the rocks and crystals that result from those processes, as described, for example, by Carmichael (1969), Kretz (1974), Fisher (1978), Ridley & Thompson (1986), and Carlson (1989). The relative rates of nucleation, reactant dissolution, intergranular transport, and product precipitation ultimately determine many key features of the rock's texture and of the zoning of porphyroblasts within it, so measurements of those features can provide information on mechanisms of crystallization.

Conceptual models of crystallization provide the link between measurable textural and chemical features in a rock and the mechanisms that produced them. One end-member model is the case of diffusion-controlled growth, in which the growth rate of porphyroblasts is limited by the kinetics of diffusional transport of components from the reactants to the growing crystal through the intergranular medium. Another end-member model is the case of interface-controlled growth, in which diffusional transport is sufficiently rapid to continually provide all crystals with the components needed for their growth, so that the growth rate of porphyroblasts is limited instead by the kinetics of attachment of components at the surface of the growing crystal.

As described in detail in the literature cited above, careful analysis of porphyroblastic rocks allows us to discriminate between these two possibilities, because diffusion-controlled growth of porphyroblasts has several important textural and chemical consequences that do not arise in the case of interface-controlled growth. First, the development of diffusionally depleted zones reduces the chemical affinity for reaction around each growing crystal, leading to local suppression of nucleation; this reduction produces a tendency toward spatial ordering of the porphyroblasts. Second, diffusional competition for nutrients among neighboring porphyroblasts reduces fluxes of nutrients for crystals in close proximity to one another, leading to local suppression of growth; this reduction produces a tendency for porphyroblasts in close proximity to be smaller than those that are more isolated. Third, the requirement in diffusion-controlled growth that nutrients be drawn from progressively more distant sources over time (contrasted with the interface-controlled situation in which all crystals draw nutrients locally from a uniform rock-wide reservoir) leads to rates of radial growth that decrease with time in the case of isothermal growth; this reduction yields systematic relationships in the patterns of chemical zoning for crystals over a range of sizes that

are distinct from those predicted for interface-controlled growth. Fourth, variations in rates of intergranular diffusion among components make possible a wide array of chemical effects at the surface of the growing crystal, with elements that diffuse more rapidly than the dominant growth-controlling component equilibrating over large length-scales, and progressively slower-diffusing elements equilibrating over a range of progressively smaller length-scales. In the growing porphyroblasts, these variations yield chemical zoning that for some elements may be controlled by intensive parameters and expressed rock-wide, but for other elements may be controlled wholly by compositional variations in the immediate vicinity of the growing crystal.

Geological Setting

The principal focus of this study is a regionally metamorphosed paragneiss from the vicinity of Passo del Sole, near Lukmanier Pass in the central Swiss Alps, which contains numerous porphyroblasts of garnet that grew during heterogeneous shearing. After a brief investigation of the field setting of this gneiss, a detailed analysis was undertaken of crystallization mechanisms within one hand sample of it that contains garnet crystals with unusually complex compositional zoning.

Regional and local geology

Lukmanier Pass lies approximately 75 km southeast of Lucerne, Switzerland, on the border of the cantons of Ticino and Graubünden. It is located on the northern edge of the pre-Mesozoic Lucomagno nappe and just south of the Gotthard massif. The area around the pass exposes the transition zone from greenschist-facies assemblages in the north to amphibolite-facies assemblages in the south, and represents peak-metamorphic conditions of approximately 500–550°C at 5 kbar (Adams *et al.* 1975, Fox 1975, Frey 1978, Frey *et al.* 1980).

Rocks near Lukmanier Pass have experienced at least three phases of Alpine deformation that correlate with the deformation in the rest of the Lepontine area (Chadwick 1968, Thakur 1973, Milnes 1976, Rosenfeld 1978, 1987). The first phase consisted of early thrusting that folded and imbricated the basement and sedimentary cover units. The second phase created large regional folds, including the Piora and Molare synclines, and developed the main penetrative foliation, which strikes east–west and dips steeply north. The third phase produced a weak crenulation cleavage and small-scale folds whose axial planes strike southeast and dip shallowly to the northeast, with fold axes plunging shallowly to the east-southeast. Metamorphism in the area began during the second phase of deformation, but peak conditions and major growth of minerals (regionally: chlorite, garnet, staurolite, kyanite, plagioclase, and hornblende) occurred during the third phase of deformation.

Sample description

Passo del Sole, which straddles the Piora Syncline approximately 3 km south-southwest of Lukmanier Pass, hosts exposures of the Orange Gneiss of Chadwick (1968), in contact with the Mesozoic metasedimentary cover rocks of the Gotthard Massif. The location of Passo del Sole in coordinates of the Swiss National Grid (CH 1903 datum) is 702204 × 154288. In one sample of the Orange Gneiss, collected by Dr. John Rosenfeld in 1963 approximately 40 meters south of the crest of the pass (Adams *et al*. 1975), we found synkinematic garnet with unusually intricate Ca zoning. For comparison with that sample (which was designated AG4), we collected 12 additional samples of the Orange Gneiss from the vicinity of Passo del Sole in 2001. (Unfortunately, the original outcrop from which AG4 was collected no longer exists; at some time between 1963 and 2001, it was obliterated by the emplacement of a small tunnel.) Compositional zoning in garnet was found to be highly variable from one sample to another, particularly for Ca. None of the samples collected in 2001, however, possesses Ca-zoning with the strikingly informative character of that in AG4; those samples thus are not described in detail here.

Sample AG4 is a porphyroblastic micaceous gneiss with prominent crystals of garnet 2 to 10 mm across in a foliated matrix dominated by quartz, white mica, and biotite (Fig. 1). The assemblage also includes small amounts of staurolite, kyanite, plagioclase, rutile, and ilmenite, and trace amounts of allanite and zircon. Discontinuous layers of polycrystalline quartz (0.1 to 6 mm wide), conformable to the foliation, are common. Secondary chlorite forms a partial rim on some garnet crystals and occurs as laths in the matrix, with long axes of crystals in thin section set at a high angle to the foliation.

Garnet varies in occurrence through the sample, ranging from isolated crystals to small clusters of crystals concentrated along single layers in the foliation. Garnet crystals commonly contain elongate inclusions (mostly quartz) that define sigmoidal patterns, although the abundance, orientation, and degree of alignment of the inclusions vary from crystal to crystal. Smaller porphyroblasts of staurolite are present, some with sigmoidal trails of inclusions. Rare crystals of kyanite are found in contact with staurolite; simultaneous extinction for both phases indicates that they bear a topotactic relationship to one another. Plagioclase is sparsely and heterogeneously distributed throughout the sample as large (~1 mm), anhedral, elongate crystals, with long axes aligned parallel to the foliation.

No lower-grade equivalents of this unit exist in the area, so the precise reaction responsible for garnet crystallization cannot be ascertained. Nonetheless, insofar as sample AG4 is not unusual in terms of its bulk composition, garnet production should be well approximated by the model reaction Ms + Chl + Pl + Qtz = Grt + Bt +

H_2O. There is no evidence for appreciable dissolution and regrowth of garnet during its crystallization interval. Such processes would be unexpected, given the very small modal amounts of phases whose growth might require garnet breakdown (staurolite: <2%, kyanite: <1%); the well-defined euhedral growth-banding made evident by compositional zoning (see below) rules out significant resorption of garnet other than late-stage peripheral retrogression to chlorite.

Sample AG4 was chosen for this study because its garnet crystals were known to contain sigmoidal trails of inclusions that provide evidence for syndeformational growth (Rosenfeld 1987). The origin of curved trails of inclusions is controversial. Many investigators believe that they indicate that the porphyroblasts rotated during growth (*e.g.*, Rosenfeld 1970, Schoneveld 1977), whereas others suggest that the foliation rotated about the porphyroblasts (*e.g.*, Bell 1985, Bell & Johnson 1989). For the purpose of this study, the distinction is not critical; under either interpretation, the sigmoidal patterns indicate garnet growth during active deformation, as opposed to static overprinting of a pre-existing fabric.

In sample AG4, individual crystals of garnet display a variety of types of inclusion trails, even when all are viewed on sections cut carefully through the morphological centers of crystals and perpendicular to rotation axes. Inclusions that make up the trails are dominantly quartz, but allanite, ilmenite, zircon, titanite, apatite, and rare tourmaline also were found. Some porphyroblasts contain abundant inclusions defining a strong sigmoidal pattern, whereas others contain relatively few inclusions with little or no alignment. In garnet crystals containing sigmoidal trails of inclusions, the quartz inclusions are parallel and straight in the central portions of the porphyroblasts, indicating that the garnet cores overgrew a pre-existing planar foliation in the early stages of their crystallization. Outside the core region, inclusion trails are curved to varying degrees, with maximum rotations in excess of 180°. Near the rim, the inclusion trails in many cases straighten into a new orientation. The outermost portion of the rim is commonly inclusion-free.

The varying degree of curvature and changing orientation of the inclusion trails throughout the specimen indicate that the outer portions of the garnet crystals grew during heterogeneous shearing. Although the foliation is weakly crenulated, the crenulations are not oriented parallel to the curved trails of inclusions. The matrix foliation wraps around garnet porphyroblasts. Discontinuity between interior and exterior fabrics indicates that garnet did not overgrow a pre-existing crenulation cleavage. Instead, the weak crenulation cleavage developed during and after garnet growth.

Analytical Methods

Determination of mechanisms controlling garnet crystallization requires precise knowledge of the porphyroblasts' spatial locations and sizes in three dimensions, and complete information on chemical zoning extending from each crystal's center of nucleation to its outer rim. Relationships between crystal growth and deformation are revealed most clearly on sections that are oriented perpendicular to the crystal's axis of rotation during growth and that pass through its nucleation center. High-resolution X-ray computed tomography (HRXCT) provides a rapid, accurate and non-destructive means to locate and measure garnet porphyroblasts. It also determines explicitly the proper position and orientation of central sections through porphyroblasts to be used for analysis of the geometry of their inclusion trails and for electron-probe microanalysis (EPMA) of their patterns of chemical zoning.

High-resolution X-ray computed tomography

HRXCT produces three-dimensional (3D) grayscale images in which contrast corresponds closely to density differences, so it is ideally suited for quantitative analysis of porphyroblastic textures (Carlson & Denison 1992, Denison & Carlson 1997, Ketcham & Carlson 2001). A hand sample of specimen AG4 was scanned in the HRXCT facility at the University of Texas at Austin. The imagery, which permitted the assessment and measurement of each garnet crystal's size, shape, degree of isolation, and inclusion density, was used to provide data for statistical measures used in quantitative textural analysis and to select optimal crystals for EPMA.

Because the 3D image may be digitally resliced in any orientation, the HRXCT data were reoriented for viewing on sections perpendicular to the axis of rotation of the garnet crystals, which are revealed in the HRXCT imagery as the sections displaying maximum curvature of the inclusion trails (Rosenfeld 1970). The central section through any garnet crystal could then be located by identifying the slice containing the maximum cross-sectional area perpendicular to the rotation axis. Even though many of the crystals are not spherical, this section was chosen as the one most likely to contain the nucleation site; as shown below, the Ca-zoning patterns in sample AG4 are so intricate and systematic that the few slightly off-center sections that were encountered were easily recognized. After scanning, two small blocks (each approximately $2 \times 3 \times 5$ cm) were cut from the sample, and using the HRXCT scans as a guide, each was ground to within 0.25 mm of a selected porphyroblast's central slice, then polished for EPMA.

After chemical mapping and analysis, each block was ground further to reveal the central section through the next selected garnet crystal, and so on. A total of 20 carefully selected and precisely positioned central sections were prepared in this way.

Electron-probe micro-analysis

Qualitative compositional X-ray maps were made to assess the overall character of the garnet zoning and to determine the best location for subsequent quantitative analyses. With the JEOL 733 Superprobe used for this study, X-rays maps were produced by rastering the electron beam across small contiguous areas of the garnet crystal, then assembling those rastered images into a mosaic grayscale image that shows qualitatively the distribution of an element across the garnet section. In each X-ray map, brighter grayscale values correspond to higher elemental concentration; however, the same grayscale value may represent slightly different concentrations in different X-ray maps, because the X-ray intensity for each map is scaled independently. Garnet crystals were mapped for major-element concentrations (Mn, Mg, Fe, and Ca) using identical operating conditions of 15 kV accelerating voltage, 500 nA sample current on brass, and a 50 ms dwell time. The resolution of the images was dependent on the size of the crystal, and ranged from 5 to 11 μm/pixel. Grayscale levels were adjusted in Adobe Photoshop® for better visualization of the elemental zoning.

Quantitative analyses were obtained along linear traverses positioned to include the core (nucleation site) and rim of the crystals, avoiding as many inclusions as possible in areas with complex compositional zoning. In addition, some shorter traverses were performed at higher spatial resolution across regions with complex compositional zoning. All of the traverses were automated and included analysis of the crystals for Si, Al, Mn, Fe, Mg, Ca, and Ti. Data were acquired by wavelength-dispersive techniques, with 20 s analysis times, 15 kV accelerating voltage, and a 20 nA sample current on brass. Standardization was performed on silicate min-

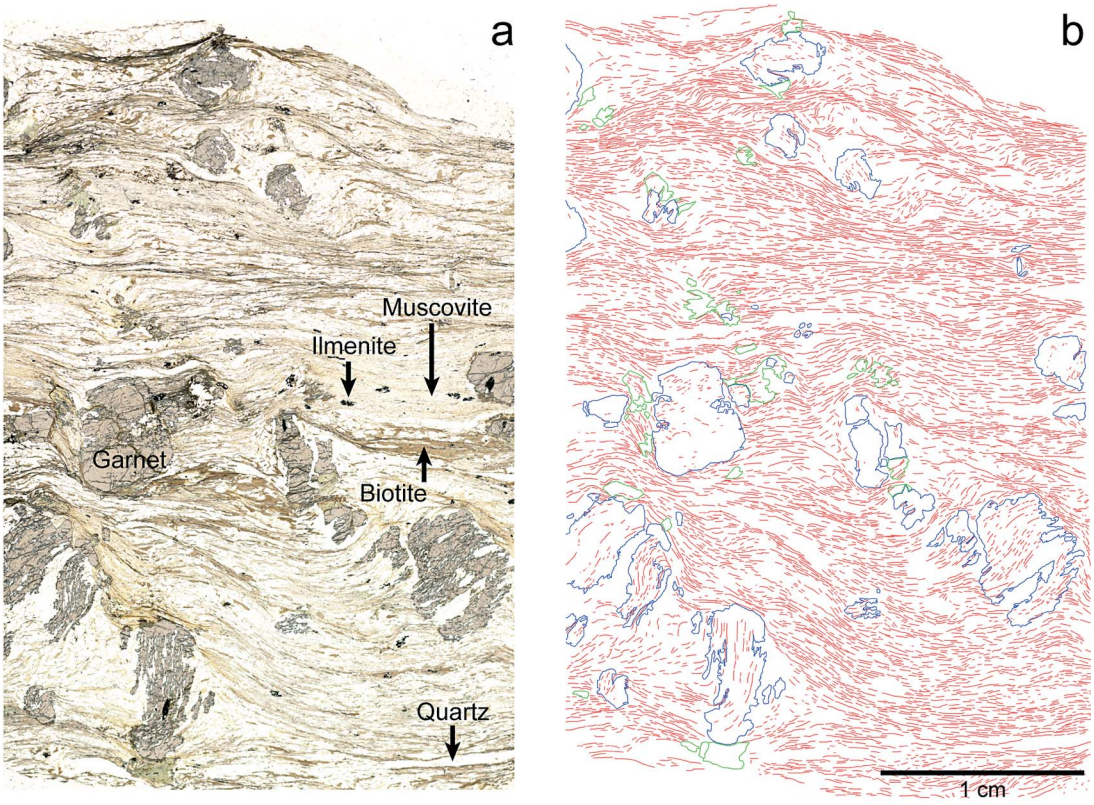

FIG. 1. (a) Thin-section view (uncrossed polars) of sample AG4. (b) Tracing of microstructures documenting synkinematic growth. Foliation and inclusion trails are traced in red, garnet crystals are outlined in blue, and staurolite and kyanite crystals are outlined in green.

erals and glasses; data reduction employed a ZAF correction.

Quantitative Textural Analysis

Quantitative textural analysis (QTA) provides a means of identifying the operation of a variety of crystallization mechanisms in porphyroblastic rocks (Carlson 1989, Denison *et al.* 1997, Hirsch *et al.* 2000). One approach employed in QTA is the comparison of statistical analyses of HRXCT data on the sizes and locations of porphyroblasts with statistics derived from numerical simulations of interface-controlled processes. In such comparisons, we seek evidence for diffusion-controlled nucleation and growth in the form of statistically significant spatial ordering of crystal centers, or correlations between crystal size and degree of isolation, or both. The same statistical measures will also identify clustering effects that can result from local concentrations of nucleation sites; if such effects are pronounced, they may obscure the signal that characterizes diffusion-controlled growth.

Results

The HRXCT approach provided precise measurements of the sizes and locations of 1,348 garnet porphyroblasts in a hand-sample-sized volume of specimen AG4. These data were used to evaluate scale-dependent correlation functions that provide information on the macroscopic textural effects of contrasting mechanisms of crystallization (Raeburn 1996, Daniel & Spear 1999, Hirsch *et al.* 2000). Two correlation functions have proven particularly useful for QTA. The first is the Pair Correlation Function (PCF) with minus sampling; it describes the degree of departure from randomness in the spatial disposition of crystals, which tests for the superposed effects of suppressed nucleation in diffusionally depleted zones surrounding growing crystals and clustering of potential sites of nucleation. The second is the Mark Correlation Function (MCF); it describes the degree of departure from randomness in the sizes of near-neighbor crystals, which tests for growth suppression resulting from diffusional competition for available nutrients among crystals in close proximity to one another. The values of the PCF and MCF for sample AG4, computed according to the methods of Hirsch *et al*. (2000), are compared in Figure 2 to the 95%-confidence envelope that indicates the range of expected variation for an interface-controlled process operating in a rock with a homogeneous disposition of potential sites of nucleation.

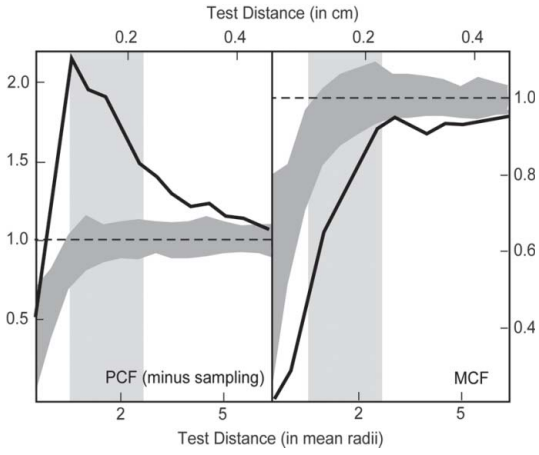

FIG. 2. Correlation functions computed from HRXCT data. Lighter shading indicates range of test distances corresponding to one standard deviation on each side of mean nearest-neighbor distance. Darker shading represents 95% confidence interval for functional values obtained for interface-controlled processes in a rock in which potential sites for nucleation are homogeneously distributed. PCF values above the shaded region result from strong clustering of potential sites for nucleation. MCF values below shaded region reflect growth suppression of nearby crystals resulting from diffusional competition for nutrients.

Interpretation

Values for the PCF fall above the 95%-confidence envelope. This result is not surprising, as it reflects the strong clustering of potential nucleation sites in sample AG4, visible at several scales. Garnet crystals in AG4 are localized along foliation layers throughout the sample. Within a single layer, garnet crystals are commonly restricted to certain parts of the layer, whereas other parts of the same layer are garnet-free. The X-ray compositional maps described below also reveal that some porphyroblastic masses represent coalescence of crystals growing from multiple closely adjacent centers of nucleation. Thus in this sample, strong clustering obscures any possible underlying signal in the PCF that might indicate partial ordering of crystal centers due to diffusionally depleted halos surrounding earlier-nucleated crystals.

Values for the MCF, at the relevant length-scales corresponding to the mean nearest-neighbor distance and just beyond, fall well below the 95%-confidence envelope. This indicates that in sample AG4, garnet crystals with close neighbors are significantly smaller than garnet crystals that are more isolated, an expected consequence of diffusional competition for nutrients during growth. It is not surprising that the MCF indicates growth suppression even though the signal for nucleation suppression in the PCF is overwhelmed by clustering: the ability of the MCF to detect diffusion-controlled signals even in clustered arrays of crystals has been well documented (Hirsch *et al*. 2000).

Discussion

An underlying assumption of this type of textural analysis is that the crystal centers have not moved appreciably, relative to one another, since their nucleation. Garnet in AG4 grew during backfolding of the surrounding nappes (Rosenfeld 1978), so heterogeneous shearing of the sample during the recumbent folding might have displaced the crystals from their original relative positions. The amounts of any such displacements are unknown. But to alter the MCF so as to yield a false diffusion-controlled signal, movements during shearing would have to preferentially group together smaller crystals while preferentially separating larger crystals, an unlikely possibility.

A further complication arises from the fact that *compound* crystals, those that originate from two or more nuclei that grow into coalescence, were not always easily recognized in the HRXCT data, making it likely that in some instances, multiple crystals were regarded as a single porphyroblast. Similarly, the strong clustering of garnet crystals made it difficult in some cases to identify individual crystals in the centers of the clusters. These errors cause the number of nucleation events to be underestimated and the sizes of crystals to be overestimated. The magnitude of these effects on the correlation functions is not known, but they would tend to skew the MCF toward lower values, possibly falsely enhancing the diffusion-controlled signal.

Although the PCF is dominated by the clustering effect and thus provides no further information, and despite complications in the MCF calculation, quantitative analysis of the porphyroblastic texture in sample AG4 supports the conclusion that the sizes and locations of its garnet crystals were governed by a diffusion-controlled nucleation-and-growth process.

Patterns of Zoning in Garnet: Observations

Garnet in sample AG4 is almandine-rich but highly zoned, spanning the range $Sps_{1–20}Prp_{5–16}Alm_{63–74}Grs_{9–12}$, corresponding to 0.2–8.9 wt.% MnO, 1.2–3.5 wt.% MgO, 27–36 wt.% FeO, and 3.1–6.4 wt.% CaO. Zoning patterns show banding with euhedral shapes, made particularly evident by sharp oscillations in Ca content, and thus can be unambiguously interpreted as preserved growth-zoning (Figs. 3–5).

X-ray compositional maps reveal three categories of growth features differentiated by the location and number of nucleation sites. Because the plane of each X-ray map passes through the center of the porphyroblast, the point at the center of the concentric Ca oscillations is inferred to be the site at which the crystal nucleated. *Normal* porphyroblasts are those for which the nucleation site is approximately in the morphological center of the analyzed section through the garnet crystal (Fig. 3). *Partial* porphyroblasts are those for which the nucleation site is in close proximity to one edge of the crystal, so that the majority of growth took place to one side of the nucleation site (Fig. 4). The zoning patterns and external shapes of these crystals have the appearance of being truncated along the side closest to the nucleation site. This "truncated" side is invariably adjacent to a large layer of monomineralic quartz. *Compound* porphyroblasts are those for which multiple sites of nucleation are apparent from the zoning patterns, although at least some of the Ca oscillations enclose all the nucleation sites (Fig. 5). These porphyroblasts are interpreted to represent polycrystalline aggregates of two or more initially separate crystals that impinged during their growth.

Normal crystals of garnet display a bell-shaped profile of Mn, with a high-Mn core and low-Mn rim, accompanied by gradual increases in Fe and Mg toward the rim. In contrast, *compound* and *partial* crystals diverge from this pattern, with Mn displaying an initial rimward increase (decreases for Fe and Mg), before reversing this trend and decreasing rimward (increases for Fe and Mg). Even more extraordinary is the complex Ca zoning. Concentrations of Ca increase gradually away from the core of the crystals for roughly half of the total radius, but numerous fine-scale oscillations are found in more distal portions of the crystals, and a discontinuous high-Ca zone comprises the outermost rim. Patterns of Fe and Mg zoning are broadly similar to one another but generally antithetical to Mn and Ca zoning. These characteristics are described in greater detail below.

Mn zoning

Of the 20 garnet crystals that were mapped on central sections, 12 display a monotonic decrease in Mn content toward the rim, with a bell-shaped profile. For crystals of this type, MnO at the nucleation site ranges from 5.9 to 8.9 wt.%, with higher concentrations corresponding to crystals with larger radii. Edge compositions vary considerably along the perimeter of a single crystal because some crystal faces (or parts of crystal faces) that impinged on quartz pods stopped growing before the overall cessation of garnet growth. In addition, some edges have been resorbed during retrogression to produce a rim of chlorite. Analyses of unimpinged, unresorbed rims average 0.25 wt.% MnO.

Patterns of manganese distribution for the remaining eight crystals show unexpected features; in particular, their nucleation sites do not correspond to their highest Mn contents. From the nucleation site outward, Mn content increases to a maximum, then reverses to establish a normal profile of a decrease to the rim (Fig. 5). This reversal occurs in every *partial* crystal and every *compound* crystal, but is not seen in *normal* crystals. Compositions at the site of nucleation of crystals containing a Mn reversal range from 4.6 to 8.3 wt.% MnO; the higher central Mn contents are commonly found in larger crystals. Rim compositions are similar

to those in garnet crystals with bell-shaped zoning profiles.

Ca zoning

Garnet from sample AG4 displays complexities of Ca zoning that are rarely observed in crystals of regional-metamorphic garnet. The pattern is intricate, yet virtually identical in every crystal regardless of its size (Fig. 6). Calcium is low at the nucleation site (ranging from 3.5 to 5.1 wt.% CaO) and increases gradually outward. It drops slightly over a narrow interval before escalating steeply to a sharp "Ca spike" that stands out as a dominant feature in the Ca X-ray maps (Fig. 6). The sides of this dominant Ca spike are typically symmetrical and very steep, encompassing changes as large

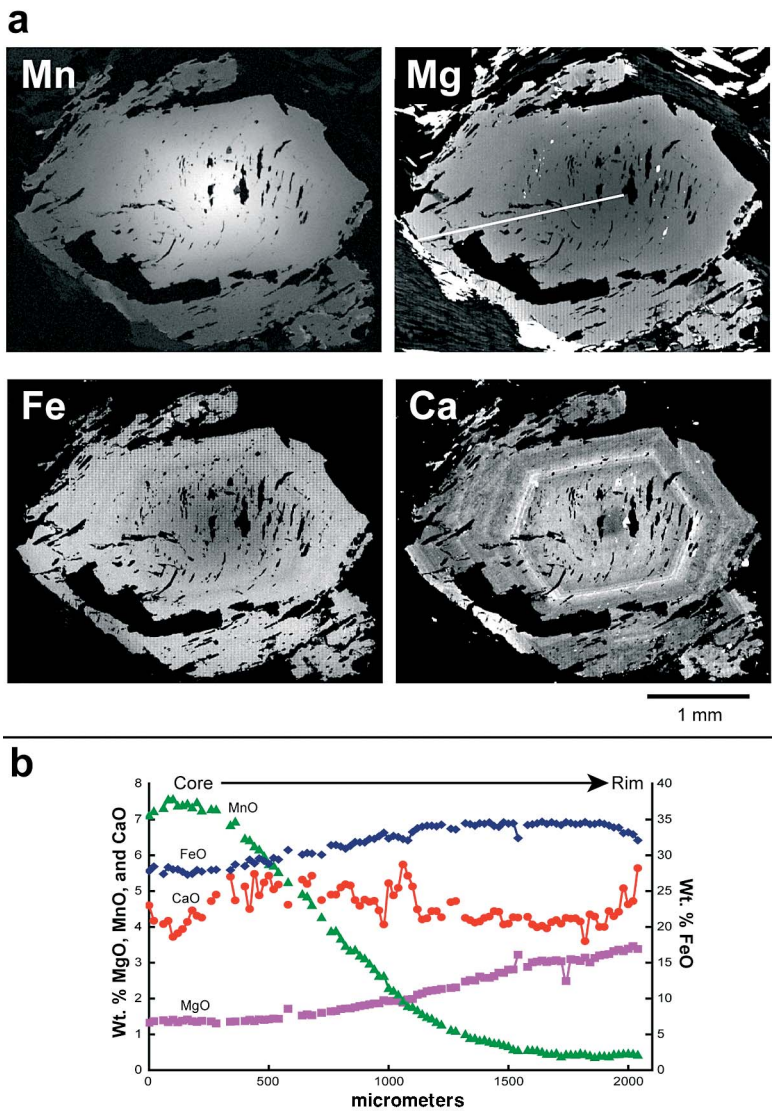

FIG. 3. (a) EMPA X-ray compositional maps of central section through Garnet 18. Higher concentrations are brighter. In this *normal* garnet, Mn concentrations decrease monotonically from core to rim. The euhedral character of interior banding indicates that zoning originated during growth. Note sigmoidal trails of inclusions. (b) Results of EMPA analyses along traverse are marked by white line on Mg X-ray map.

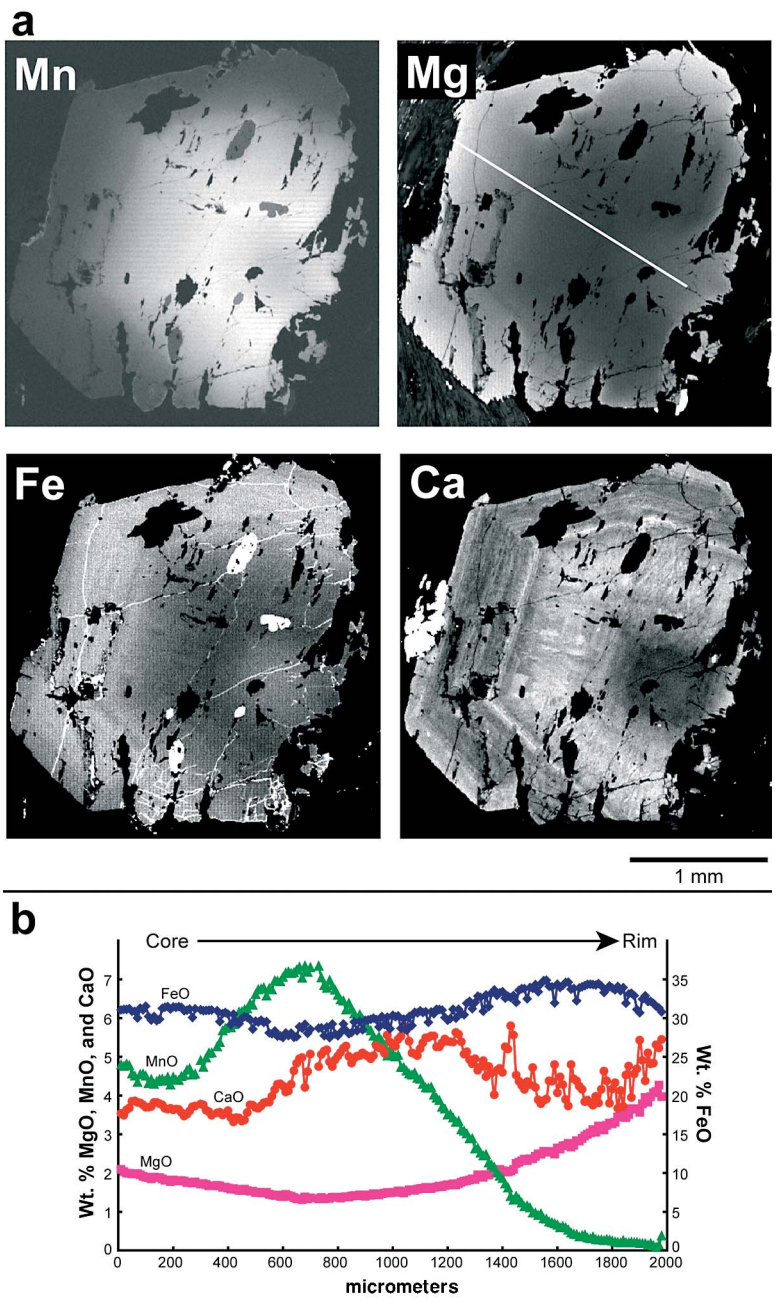

FIG. 4. (a) EMPA X-ray compositional maps of central section through Garnet 10. Higher concentrations are brighter. In this *partial* garnet, Mn concentrations at the nucleation site are not the highest in the crystal; instead, Mn concentrations rise outward from the nucleation site, reach a maximum at an intermediate radius, then decline to minimum values at the rim. Fe and Mg show variations antithetical to Mn, but Ca zoning follows the same pattern seen in *normal* crystals of garnet. (b) Results of EMPA analyses along traverse marked by white line on Mg X-ray map.

as 1.7 wt.% CaO (an increase of 38%) across as little as 30 μm. On the side of the Ca spike nearer the nucleation site, two smaller spikes are found, each one stepping progressively higher until the dominant Ca spike is reached (Fig. 7). The rimward side of the main Ca spike is the margin of a wide zone composed of fine-scale Ca oscillations, many of which are less than 10 μm wide (Fig. 7). The resolution of the X-ray maps relative to the thickness of the oscillations makes the narrower oscillations difficult to correlate exactly from one crystal to another, but there are two particularly high peaks within the oscillatory zone that are easily identified in every crystal. A high-Ca zone, seen as a bright edge on the X-ray maps, comprises the outermost rim of the garnet crystals. This rim is highly discontinuous, present only where garnet is adjacent to micaceous portions of the matrix, and absent where garnet is in contact with matrix quartz.

Fe and Mg zoning

In *normal* garnet crystals, Fe and Mg are relatively low at the nucleation site and increase rimward. For these crystals, compositions at the nucleation site range from 27.4 to 28.9 wt.% for FeO and from 0.2 to 1.4 wt.% for MgO. The ratio Fe/(Fe+Mg) decreases from the nucleation site toward the rim, as expected for garnet crystallizing with increasing temperature. In *partial* or *compound* crystals (those displaying a Mn reversal), Fe and Mg are likewise anomalous: their nucleation sites do not correspond to their lowest concentrations of Fe and Mg. Instead, Fe and Mg contents are relatively high at the nucleation site and decrease outward to a minimum, after which they increase normally to the rim. The minimum in the Fe and Mg zoning is at the same location as the Mn maximum. For these crystals, core compositions range from 28.5 to 30.2 wt.% FeO and from 1.3 to 2.8 wt.% MgO.

Patterns of Zoning in Garnet: Implications for Mechanisms of Crystallization

Patterns of garnet zoning in sample AG4 reveal a quantitative proportionality between the radii of garnet crystals and their radial rates of growth, a relationship not previously documented for porphyroblasts. That relationship is interpreted here as the consequence of diffusion-controlled crystallization from a heterogeneous precursor. To justify that interpretation, in the following discussion we first establish that correlated Ca oscillations in garnet formed contemporaneously, then exploit that fact to extract from the Ca and Mn zoning patterns of multiple crystals a direct proportionality between growth rates and radii, and finally deduce the mechanism underlying this proportionality. This mechanism, which must be fundamentally different from the cause of size-proportional growth in some other geological systems, is diffusion-controlled growth from a heterogeneous precursor.

Contemporaneity of Ca oscillations

Distinctive Ca oscillations produce zoning patterns that are essentially identical in all garnet crystals, regardless of size. Although the detailed equivalence of Ca zoning patterns makes it seem likely that each zone formed at the same time in all crystals, that observation alone is insufficient to justify the conclusion that the zones are contemporaneous. A counterexample is found in the work of Chernoff & Carlson (1997), who described Ca spikes in garnet from the Picuris Range, New Mexico, that are very similar in appearance to the dominant Ca spike in sample AG4. The Ca spikes in the garnet crystals of the Picuris Range, however, could not have formed simultaneously. Mn, Fe, and Mg concentrations in those crystals are strongly correlated with one another (but uncorrelated with Ca concentrations); their values provide a single consistent index for time during the crystallization interval. Judged against that index, Ca spikes were generated in porphyroblasts of progressively smaller size at progressively later times throughout the crystallization interval, yet at the same time in all porphyroblasts of the same size. Thus Ca spikes in garnet crystals of the Picuris rocks reflect the local extent of reaction; they document disequilibrium for Ca at length scales larger than an individual porphyroblast (Chernoff & Carlson 1997, p. 431). Nevertheless, in sample AG4, textural and compositional evidence suggests that correlated Ca spikes are indeed contemporaneous in all crystals. The evidence presented below for contemporaneous Ca zones will focus on the dominant Ca spike, because it is the most easily identifiable feature in the Ca zoning.

The first line of evidence is derived from the intersection of the quartz-inclusion trails with the dominant Ca spike. Many of the garnet crystals contain sigmoidal quartz-inclusion trails. The inclusions preserve a planar fabric in the core, but outward from the core, the inclusion trails bend, marking the onset of deformation. In every crystal, regardless of its size, the dominant Ca spike intersects the quartz-inclusion trails just after the trails begin to bend (Fig. 8). The Ca spike thus crystallized just after the onset of deformation, which must have been essentially simultaneous for all garnet crystals.

The second line of evidence follows from the compositions of crystals at the location of the dominant Ca spike. If the Ca spike represents a single point in time, and if at that time rock-wide chemical equilibrium for Mn, Fe, Mg and Ca was established, then the garnet composition at the Ca spike should be identical in all crystals. When testing this hypothesis, it is important to consider the expected variability in the compositional measurements. Although the dominant Ca spike is the

most easily identifiable feature in the zoning patterns, it does contain a number of irregularities. For example, the X-ray maps show that the Ca spike itself changes brightness (reflecting changes in Ca concentration) along a single former crystal face. To account for such irregularities, a comparison was made between the variability within individual crystals and the variation from one crystal to another: the variances of compositional measurements within seven individual crystals for multiple locations along the Ca spike (on different former crystal faces) were compared to the scatter among *average* compositions at the spike for multiple crystals. The variances within individual crystals were substantially equal to the variability from crystal to crystal, indicating that garnet composition at the location of the dominant Ca spike is uniform (for example, within ~0.5 wt.% CaO) for all crystals.

Relationships between crystal sizes and growth rates

The widths of compositional zones that crystallized over the same time-interval in separate crystals of garnet represent time-integrated rates of radial growth for that interval. Different relationships between rates of radial growth and crystal size arise from various possible mechanisms of crystallization. Consequently, comparison of the widths of contemporaneous compositional zones in multiple crystals of garnet can determine the mechanisms governing their crystallization. The following analysis first reveals in sample AG4 a previously undocumented relationship, one in which radial rates of growth are proportional to crystal sizes, then identifies the underlying mechanism of crystallization that is likely responsible for this relationship: diffusion-controlled growth from a heterogeneous precursor.

Relationships between radii and zone widths based on Ca zoning. Because correlated Ca oscillations in sample AG4 are contemporaneous in all crystals of garnet, they can be used as time markers that divide the growth history into several discrete and recognizable intervals. Different intervals do not, of course, necessarily represent equal periods of time. As shown in Figure 9, three major subdivisions are easily recognized: Zone 1, the portion of the crystal interior of the dominant Ca spike; Zone 2, the portion of the crystal outward from the Ca spike that contains the fine-scale oscillations, and Zone 3, the discontinuous high-Ca rim. Two of the fine-scale oscillations in Zone 2 are prominent enough to be identified easily in all crystals, allowing this zone to be further subdivided into three subzones, designated Zones 2a, 2b, and 2c. In addition, there is a narrow subzone of low Ca content just interior of the dominant Ca spike, which is designated Zone 1d. (Additional subzones designated as 1a, 1b, and 1c were definable in the interior portions of some crystals, but could not be reliably identified in all, so they are not treated further here.)

Measurements of zone widths and radii were made on Ca X-ray maps. To determine zone widths and radii, distances were measured from the nucleation site to a zone boundary or garnet rim along the growth direction, which is perpendicular to the former crystal-face represented by the euhedral growth-bands. Zone widths are simply the distances between two adjacent zone-boundaries. The radius at the time of growth of each zone is taken as the distance from the nucleation site to the midpoint between the zone boundaries. Measurements of zone widths and corresponding radii were made for each zone along every suitable former crystal-face in every crystal; former crystal faces were considered suitable for measurement only if the zone boundaries were clearly defined on the Ca X-ray maps. For *compound* porphyroblasts, measurements were made only on the subcrystal for which the central section was exposed.

Within a single crystal, slightly different radii and zone widths were measured on different crystal-faces. This reflects the fact that the plane of section, even if it passes through the center of the crystal, will not, in general, intersect the former crystal-faces (zone boundaries) at right angles. Thus the measurements made are only apparent widths and radii; they will in general be somewhat larger than true widths and radii. Apparent widths and radii were converted to true widths and radii by including measurement of the angle between two adjacent dodecahedral crystal-faces, using a method devised by Prof. Wayne Dollase of UCLA [pers. commun., 2002: see Appendix I of Meth (2002) for derivation]. For some crystals, zone widths and radii could be measured only on non-adjacent crystal faces or on a single face, and therefore could not be corrected to true measurements. In these instances, in an attempt to minimize the discrepancy between the uncorrected widths and radii and the corrected widths and radii, the face with the narrowest zone-width was chosen, as measurements for this face should be closest to the true measurements. Measurements for each zone were averaged over all faces to represent the radius and zone width in each garnet crystal.

Relationships between zone widths and radii are shown in Figure 10. The near-linear positive correlations indicate that for all zones, the radial rates of crystal growth are approximately proportional to the radii of the garnet crystals at the time of growth. The correlation is strongest for garnet crystals exhibiting features of *normal* growth. A correlation with slightly greater scatter exists for the *compound* and *partial* crystals; most of them have smaller zone-widths (slower rates of growth) for a given radius than the *normal* crystals of garnet.

Relationships between radii and zone widths based on Mn zoning. Compositional variations in Mn also carry information on the relationship between growth rates and crystal size. If chemical equilibrium for Mn was achieved throughout the sample during garnet

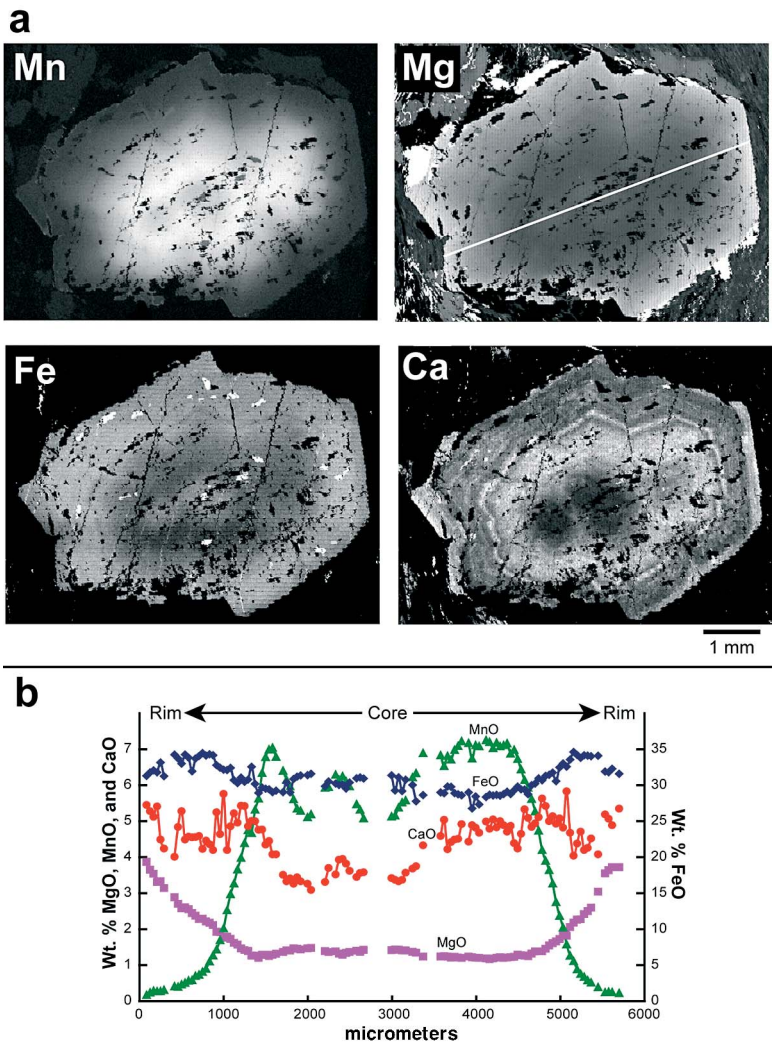

FIG. 5. (a) EMPA X-ray compositional maps of central section through Garnet 1. Higher concentrations are brighter. In this *compound* porphyroblast, three centers of nucleation are evident; the two at the left are nearly in the plane of section, but the one at the right lies just out of the plane of section. As in *partial* crystals, Mn concentrations show a maximum at intermediate radius, but Ca zoning follows the same pattern seen in *normal* crystals. (b) Results of EMPA analyses along traverse marked by white line on Mg X-ray map.

growth, then all garnet crystals in the sample would have precipitated identical values of Mn at any point in time. Zone boundaries could then be placed at selected equal values of MnO in the garnet profiles, and an analysis similar to that for Ca could be made. (Alternatively, Fe or Mg zoning could be used, as they are inversely correlated with Mn, and so would give equivalent results.)

As described earlier, however, many of the Mn X-ray maps exhibit a Mn reversal in the garnet interiors that is interpreted below to reflect local disequilibrium during the earliest stages of growth. In contrast, the equivalence of all Mn concentrations at the Ca spike indicates rock-wide equilibrium for Mn at the time of precipitation of the Ca spike. It is therefore likely that Mn equilibrium was achieved rock-wide at the time of

crystallization of the maxima in the Mn profiles, and at points rimward of the maxima. In order to avoid parts of the garnet profiles that might represent Mn disequilibrium, all Mn zones used for this analysis were chosen to lie rimward of the maximum in the Mn profile. The Mn zone boundaries were set every 0.25 wt.% from 5 to 1 wt.% MnO.

As with Ca, distances from the nucleation site to the Mn-zone boundaries were measured, but in this case, the distances were obtained not from the X-ray compositional imagery, but from EPMA line traverses. Those traverses were chosen to cross relatively inclusion-free sections of the garnet crystals, so they were generally not oriented along the growth direction (perpendicular to the former crystal-faces), but simple trigonometry suffices to convert measurements along the traverses to correct radial distances.

Zone widths and radii for the Mn zones are shown in Figure 11. As for Ca, all Mn-zone measurements display a near-linear positive correlation between zone width and radius. Although some of these slopes are numerically small, significance tests on the regression lines (Crow *et al*. 1960, p. 160) confirm that all slopes are significantly different from zero at the 95% level of confidence. The ratios of zone width to radius (the slopes of the lines in Fig. 11) increase outward from the core.

Mechanisms of crystallization

In seeking an explanation for this new finding of a direct proportionality between radius and radial rate of growth for garnet porphyroblasts, we first evaluate and eliminate mechanisms invoked by others to explain similar relationships in studies of crystal growth from aqueous solution, then consider the hypothesis that crystallization kinetics in sample AG4 are the consequence of diffusion-controlled growth from a heterogeneous precursor. Alternative mechanisms of crystallization, namely interface-controlled growth and growth governed by advective transport of nutrients, have also been

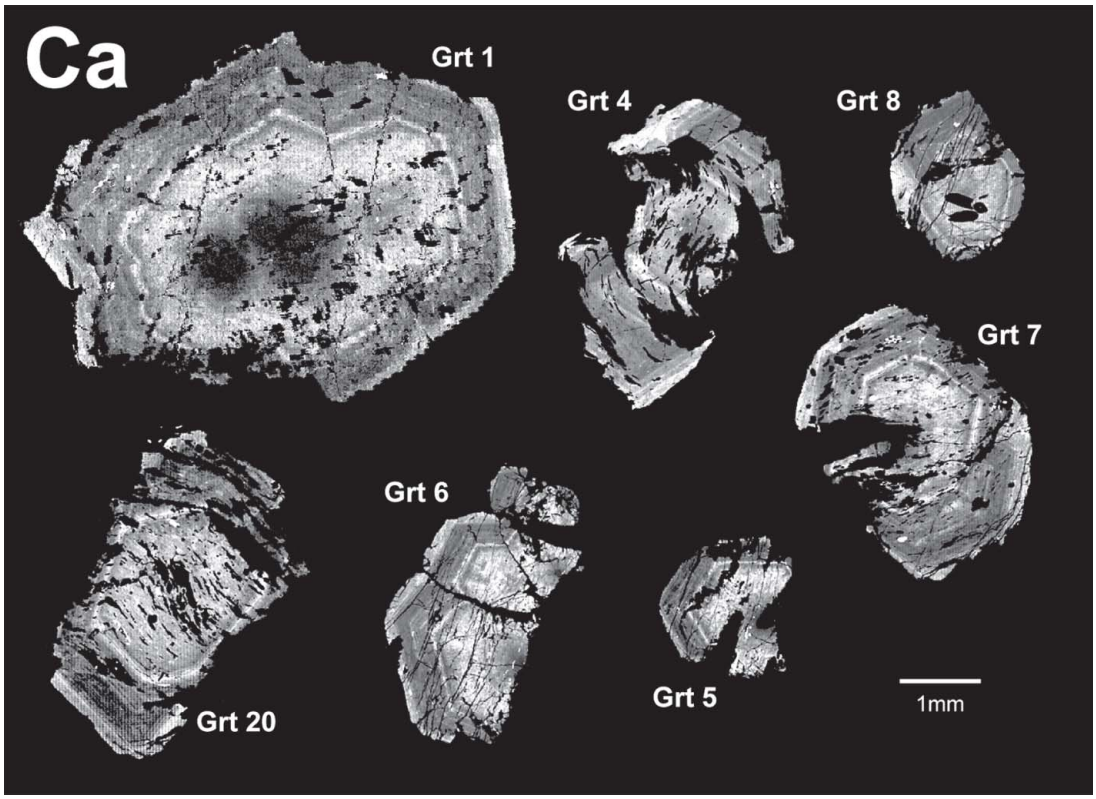

FIG. 6. EPMA X-ray compositional maps of Ca on central sections through garnet crystals in sample AG4. The same intricate pattern of zoning is observed in all crystals, regardless of size. Note, however, that brightness is scaled independently for each map, so the same concentration may appear at different levels in grayscale on different maps.

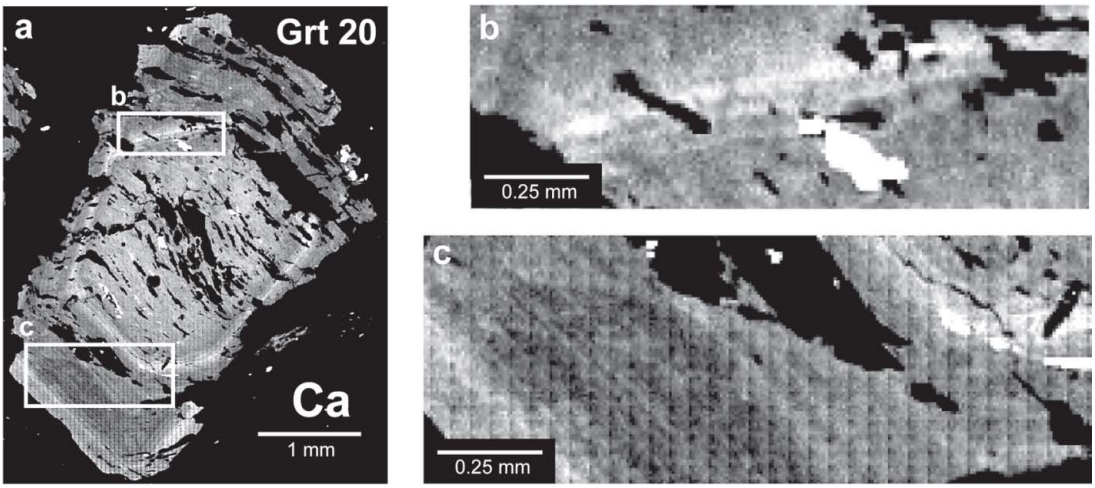

FIG. 7. EPMA X-ray compositional map of Ca on central section through Garnet 20. Part (a) locates accompanying insets. Inset (b) displays the two sharp, narrow spikes in Ca that occur just inside the dominant Ca spike. Inset (c) illustrates the very fine scale of Ca oscillations that characterize the zone outward from the dominant Ca spike.

considered, but rejected. Examination of those alternatives is postponed to the Discussion section below.

Size-dependent growth during precipitation from aqueous solution. Size-dependent (proportionate) growth has been postulated to occur during precipitation of crystals from aqueous solutions in some geological environments. Such growth has been inferred for dolomite crystallization (Nordeng & Sibley 1996), for overgrowths of diagenetic quartz in sandstones (Makowitz & Sibley 2001), and for microcline and quartz in miarolitic cavities (Kile & Eberl 1999). In laboratory circumstances, size-dependent growth has been studied in considerable detail in numerous experiments involving precipitation of crystals from solution (*cf.* Kile & Eberl 2003, and references therein). Kile & Eberl (2003) observed size-dependent growth of cm-scale crystals of alum in stirred solutions, but constant growth-rates in unstirred solutions; however, they reported size-dependent growth of μm-scale crystals of calcite in both stirred and unstirred solutions. They concluded that size-dependent growth occurs in their experiments if and only if growth is governed by the supply of reactants to the crystal surface by advective transport. At the cm scale, this occurred only in stirred solutions, but at the μm scale, they hypothesized that it occurred even in unstirred solutions because the effects of convection and Brownian motion produce solution velocities that are high in relation to the size of the very small crystals. According to Kile & Eberl (2003, p. 1515), the underlying mechanism that produces size-dependent growth in these systems is "a hydrodynamic effect that results from a faster solution velocity around larger crystals (analogous to the Bernoulli effect)."

Such hydrodynamic effects do not exist under metamorphic circumstances, in which fluid:solid ratios and fluid-flow velocities in relation to crystal size are smaller by many orders of magnitude. Instead, an alternative explanation must be sought for the direct proportionality between radius and radial rate of growth seen in this study.

Diffusion-controlled growth from a heterogeneous precursor. The QTA evidence for growth suppression of crystals in close proximity to their neighbors focuses attention on mechanisms involving intergranular diffusion as the likely rate-controlling processes for garnet growth in sample AG4. But an apparent difficulty might arise in reconciling the relationships in Figures 10 and 11 with theoretical predictions and observational confirmation (Carlson 1989, Denison & Carlson 1997) of diffusion-controlled growth rates that are inversely proportional to crystal size: for isothermal diffusion-controlled growth from a homogeneous precursor, radial rates of growth for isolated crystals take the general form $dR/dt = k_1 R^{-1}$. The relationships seen in Figures 10 and 11, however, might be considered to reflect growth-rate laws with the general form $dR/dt = k_2 R$. This ostensible discrepancy appears because the relationships in Figures 10 and 11 derive from a comparison of sizes of separate crystals growing in different environments, not successive stages in the growth of an individual crystal. The true origin of the relationships in Figures 10 and 11 becomes clear when the effect of heterogeneity in the distribution of nutrients in the precursor is explicitly considered.

If intergranular diffusion of a critical nutrient (most likely Al supplied by the breakdown of muscovite and

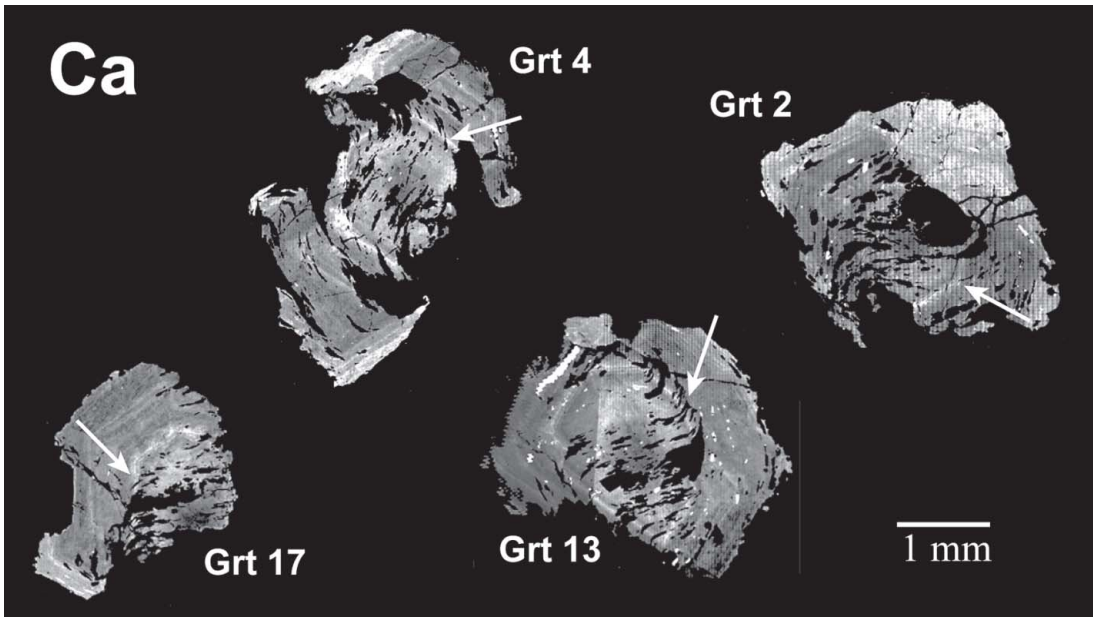

FIG. 8. EPMA X-ray compositional maps of Ca on central sections through garnet crystals in sample AG4, illustrating contemporaneity of dominant Ca spike with respect to onset of deformation, as recorded by initial bending of inclusion trails. Arrows locate intersections of the dominant Ca spike with inclusion trails that have been reoriented by small amounts in comparison to the planar fabric of inclusions in garnet cores.

chlorite) was not rapid enough to eliminate gradients in the nutrient's concentration in the intergranular medium during garnet growth, then growth rates would necessarily be controlled locally, by precursor abundance. In this circumstance, two crystals of garnet nucleating at the same time in areas with differing abundances of the critical nutrient would grow at different rates. A garnet crystal that nucleated in a region containing a greater amount of the critical nutrient would benefit from larger diffusional fluxes, and would therefore grow at a greater rate (and ultimately reach a larger size) than a garnet crystal growing in a region with a smaller amount of the critical nutrient. Thus, proportionality between growth rates and crystal size may reflect variations in local fluxes of one or more key nutrients due to heterogeneities in precursor composition, but *if and only if* heterogeneities in nutrient distribution within the precursor are sustained by sluggish diffusion through the intergranular medium. If instead diffusion were rapid enough to redistribute nutrients widely through the rock, then all growing crystals would be in chemical communication with the larger reservoir, able to draw nutrients from the rock as a whole, and crystal sizes would not depend upon the local distribution of nutrients. There is thus an important distinction between the systems described above involving precipitation from aqueous solution and metamorphic systems: in the aqueous systems, crystal size is a causative factor that directly determines growth rate by influencing the hydrodynamic flows supplying nutrients (not merely size-proportional, but size-dependent growth); in metamorphic systems, crystal size is a passive consequence of growth rates that are determined by local differences in nutrient availability.

Unfortunately, a rigorous theoretical analysis of diffusion-controlled growth from a heterogeneous precursor soon encounters daunting complexity, because when solubilities of nutrient components in the fluid are buffered by local equilibrium with reactant phases, nutrient fluxes are not directly proportional to the abundance of reactant phases that serve as nutrient sources; instead, they are complicated functions of time and distance that vary as crystallization progresses. But an informative approximation emerges if one adopts the simplification that at all times the volume of the crystal growing inside a diffusionally depleted zone is proportional to the volume fraction in that zone of the matrix phases that contribute to the crystal's growth (essentially, the local bulk-composition of the precursor). Under that assumption, diffusion-controlled growth of crystals that nucleate simultaneously and crystallize from a heterogeneous precursor will result in a positive linear correlation between radius and radial rate of growth, simply because faster-growing crystals reach greater sizes.

An illustration of that concept follows; derivations of key relationships are given in the Appendix. Consider the situation shown schematically in Figure 12, in which four crystals of garnet nucleate simultaneously in different regions of a rock, each region characterized by a different local abundance of aluminous precursor phases. The size of the diffusionally depleted zone at any time t is the same in all regions, because it is determined by the rate of intergranular diffusion of Al; the radius of the depleted zone is approximated by $R_{dpl} = (Dt)^{1/2}$, in which D is the effective intergranular diffusivity of Al. But the growing crystals will be different sizes in each region: those growing in regions richer in aluminous precursors will be larger than those growing in regions poorer in aluminous precursors, because the same depleted volume yields more nutrients in the enriched regions. The size of the crystal in each region therefore depends upon the volume fraction f of the aluminous precursor phases that contribute to garnet growth: the crystal radius is given by $R_{xtl} = f^{1/3} (Dt)^{1/2}$, and radial rates of crystal growth dR_{xtl}/dt are of course the time derivative of this expression for radius. In the isothermal case (D constant), $dR_{xtl}/dt = (1/2) f^{1/3} D^{1/2} t^{-1/2}$. In the Appendix, these expressions for R_{xtl} and dR_{xtl}/dt are combined to show that in the isothermal case, the relationship between radius and radial rate of growth for crystals grown in environments with different values of f is a line with slope $1/(2t)$.

A linear relationship also holds if temperature changes during crystal growth (so D varies with t), but in the more complicated case of prograde growth, a numerical example is more easily appreciated. This illustrative example posits simultaneous nucleation of all crystals, assigns an Arrhenius temperature-dependence to D, and models garnet growth starting at 773 K with a heating rate of 10°C/Ma; thus

$$R_{xtl} = f^{1/3} \cdot \left(D_0 \exp\left[\frac{-Q}{R(773+10t)} \right] \right)^{1/2} \cdot t^{1/2} \qquad [1]$$

Evaluating this expression and its time derivative, using values from Carlson (2002) of $D_0 = 3.0 \times 10^{-11}$ m^2/s and Q = 140 kJ/mole, yields calculated radii R_{xtl} and rates of radial growth dR_{xtl}/dt that clearly exhibit a linear relationship, as shown in Figure 12. In this prograde case, the exponential rise in diffusivity with temperature causes an increase in rate of radial growth with time for any individual crystal; if the example were isothermal, then rate of radial growth for any single crystal would decline with time and with radius as $1/R_{xtl}$.

Each individual crystal in this example obeys a diffusion-controlled rate law (Equation 1) for which the rate of radial growth (the time derivative of Equation 1) is a complex function of t. Thus the linear relationships displayed in Figure 12 do *not* represent crystals that grew in accordance with a size-proportional growth-rate law of the form $dR/dt = k_2 R$. Instead, they represent crystals that grew in accordance with diffusion-controlled growth-rate laws having the form of Equation 1, but with different values of the proportionality constant f owing to variations in precursor abundance from one

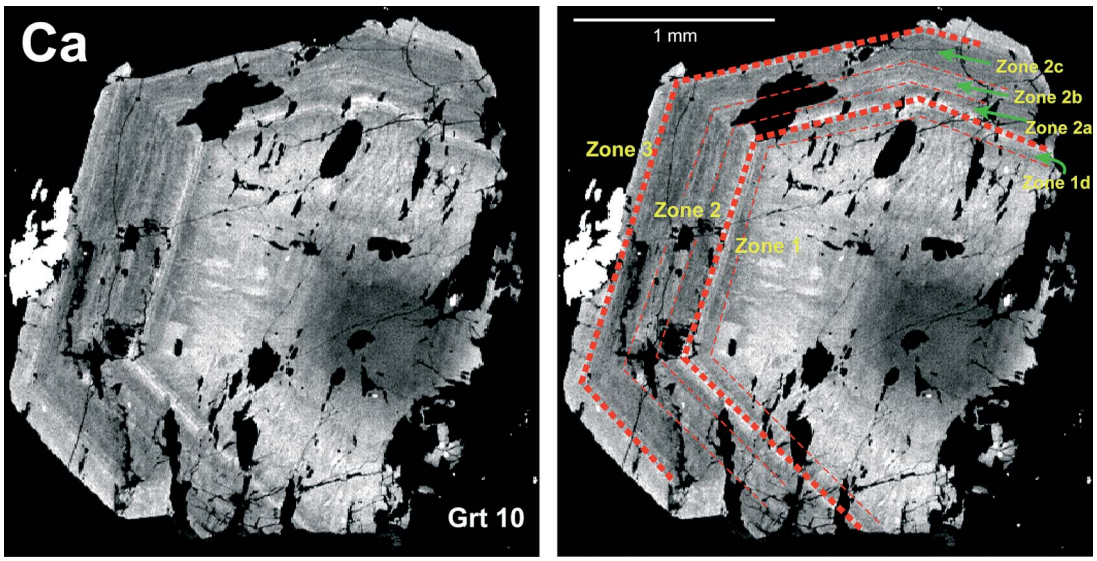

FIG. 9. EPMA X-ray compositional maps of Ca on central sections through Garnet 10, illustrating features used to delineate boundaries between contemporaneous growth-zones.

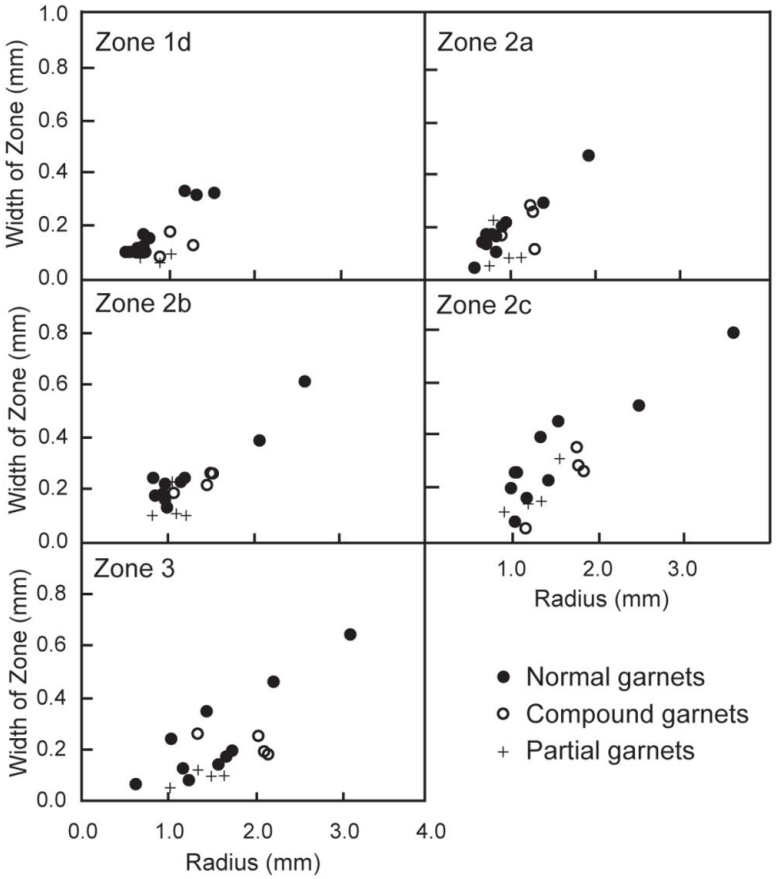

FIG. 10. Relationship between zone widths and radii for growth zones defined by Ca oscillations. Note that growth rates for *compound* and *partial* crystals mostly fall below the trends defined by *normal* crystals. Measurement uncertainties are smaller than size of plotted symbols.

region to another. Comparisons among crystals growing in different regions then exhibit the very simple relationship that faster-growing crystals attain larger sizes.

The scenario considered in the example above corresponds closely to the features observed for garnet in sample AG4. Nucleation of garnet in this rock, if not simultaneous for all crystals, was nearly so. The central Mn content in garnet is commonly used as proxy for nucleation time (*e.g.*, Carlson 1989, Chernoff & Carlson 1997), but that cannot be done in this instance, because to do so requires that Mn maintains rock-wide equilibrium throughout the crystallization interval. In sample AG4, however, Mn apparently did not achieve rock-wide equilibrium during the early stages of garnet crystallization (see Discussion below). Nevertheless, it is clear that nucleation must have occurred over a restricted time-period near the beginning of the garnet-crystallization interval, because: (1) every crystal contains the entire intricate pattern of Ca variations, including the dominant Ca spike, and (2) the relative volume of Zone 1, which is the region inside the Ca spike, as a percentage of the total volume of the crystal is very small and similar (from 6 to 15%) in all *normal* crystals. For simultaneous nucleation, diffusion-controlled growth from a heterogeneous precursor would result in relationships of the kind shown by the data for *normal* crystals in Figure 10, and by all data in Figure 11. The effects of diffusional competition, seen as a growth-suppression signal in the MCF data, will be superimposed on this general relationship. Such competition would account for the observation in Figure 10 that within a single growth-zone, zones in *compound* crystals generally have smaller widths (that is, slower growth-rates) for any given radius than *normal* crystals.

Mechanisms of crystallization of crystals that nucleate sequentially and grow within the same homogeneous matrix can be assessed using normalized radius–rate diagrams (*e.g.*, Kretz 1974, Carlson 1989, Daniel & Spear 1999), in which one plots the width of a selected compositional zone, normalized to the width of the same zone in the largest crystal, against the midpoint radius of that zone, again normalized to the midpoint radius of the same zone in the largest crystal. It is therefore natural to wonder how crystals that nucleate simultaneously and grow under diffusional control within different regions of a heterogeneous rock would appear on such a diagram, and how the crystals from Sample AG4 plot by comparison. With simultaneous nucleation and in the absence of diffusional competition, strict proportionality between radii and rates of radial growth means that the normalized radii for all zones in any one crystal are the same, and similarly, the normalized zone-widths (growth rates) for all zones in any one crystal are the same. Consequently, all zones in any crystal would plot as a single point on a normalized radius – rate diagram, instead of forming an array of points with a trajectory characteristic of a particular mechanism, as occurs in other cases. Moreover, the normalized rate and the normalized radius are numerically equal, so that in this idealized case, all normalized rates should be less than unity, and data collected from multiple crystals should all fall along the line (1,1) to (0,0). Data from Sample AG4 conform well to this prediction: they yield a very narrow range of normalized radii for any single crystal of garnet (deviating by only about ±0.05 from the central value), and yield normalized rates that are all less than unity and span a range of about ±0.2 around the line (1,1) to (0,0), that is, the values for which the normalized radius and rate are numerically equal. This dispersion of normalized rates is a predictable consequence of small differences in nucleation times and of diffusional competition among neighboring crystals.

The postulated mechanism of diffusion-controlled growth from a heterogeneous precursor also is consistent with several indications that garnet growth in sample AG4 was influenced by heterogeneities in the matrix. Commonly, garnet growth appears to have been halted by large concentrations of quartz, which of course provides little of the nutrients needed by the growing crystal; this is evident in *partial* crystals, near quartz-rich pressure shadows, and along garnet rims. At smaller scales, irregularities in the Ca zoning are also usually

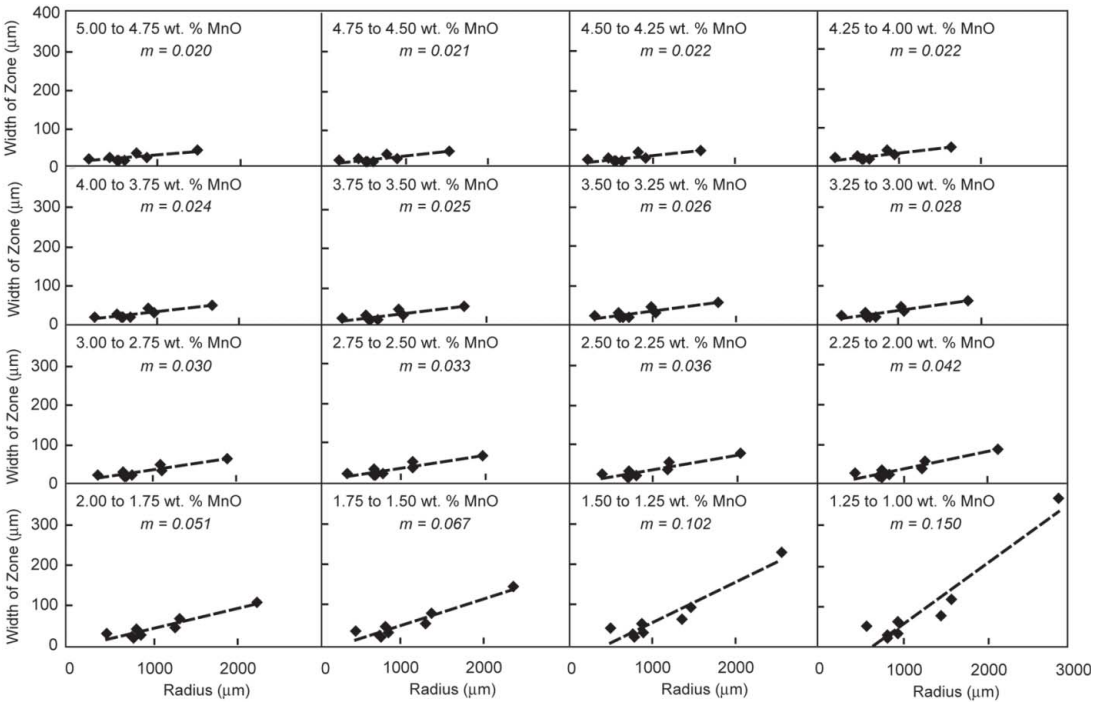

FIG. 11. Relationship between zone widths and radius for growth zones defined by intervals of Mn concentration. Dashed lines are linear regressions through the data; slopes of regression lines (values of *m*) increase systematically toward lower concentrations of Mn at crystal rims.

associated with a lack of nutrients in the vicinity of large inclusions of quartz; examples are offsets of Ca oscillations, coreward indentation of the oscillations, and reentrant angles in the oscillations, as documented in Meth (2002).

One unexpected feature of the data on zone width *versus* radius that still defies a precise explanation should be brought to light: whereas the relationship calculated in the Appendix suggests that the slopes of lines relating these quantities on diagrams like those of Figures 10 and 11 should decrease over time [slope = $1/(2t)$ in the isothermal case], the data in Figure 11 for Mn instead document an increase in slope over time. (The scatter in Figure 10 makes it unclear whether or not slopes for Ca increase.) This discrepancy may result from a breakdown of two of the simplifications underlying the derivation in the Appendix, namely that all crystals grow in isolation from one another, and that the sizes of the diffusionally depleted zones are identical for all regions.

The prediction of decreasing slopes over time ignores diffusional competition for nutrients among neighboring crystals. In reality, however, during the later stages of growth, when diffusionally depleted zones surrounding the growing crystals impinge and coalesce, diffusional competition will diminish growth rates. The effects of this competition will be manifested earlier and more intensely in regions of the rock in which nutrients are scarce (which are therefore the regions in which crystals are smaller). This is because as long as any of the precursor phase remains in the vicinity of the growing crystal, the intergranular concentration of the key nutrient will be buffered to its local saturation-value in the matrix. In other words, the diffusionally depleted zone is actually the volume surrounding the crystal from which all precursor material has been removed by reaction, which will expand outward more slowly in regions with a higher abundance of precursor phases.

The reduction in growth rates due to diffusional competition would therefore be more pronounced for smaller crystals than for larger ones, which would have the effect of increasing the slopes of plots for zone width *versus* radius. Conceivably, the slope changes seen in Figures 10 and 11, relatively constant slopes for garnet interiors followed by comparatively rapid increases in slopes for garnet rims, could result from the opposing effects of the time factor (acting to decrease slopes) and the competition factor (acting to increase them). Early in the process, these factors might be closely counterbalanced, leading to small changes in slope over time; but later in the process, near the end of the crystallization interval, when coalescence of diffusionally depleted zones becomes pronounced, the competition factor might become dominant, producing a sharp increase in slopes.

Discussion

Inferred origins of zoning patterns

Origin of Mn zoning patterns. The most striking feature of the zoning patterns for Mn is the presence of annular (non-central) Mn maxima in all *partial* and *compound* crystals of garnet, and the absence of these features in all *normal* crystals. In seeking an origin for these features, the first question to consider is whether the reversal is recording rock-wide changes in Mn or whether it represents local disequilibrium. Manganese equilibration can be evaluated by comparison of two zoning profiles, that of Garnet 10, which contains a Mn reversal, and that of Garnet 14, which does not (Fig. 13). Garnet 10 contains 4.5 wt.% MnO in its core, which increases to 7.3 wt.% MnO at an internal maximum, and then decreases to the rim; the Mn profile for Garnet 14 is bell-shaped, with a core value of 8.9 wt.% MnO. If the Mn reversal reflects rock-wide equilibrium with an intergranular fluid, then portions of garnet crystals anywhere in the rock that were crystallizing simultaneously should have identical compositions. This equilibrium scenario requires that garnet crystals containing the Mn reversal must have nucleated before garnet crystals without a Mn reversal: in this example, Garnet 10 must have nucleated before Garnet 14; otherwise Garnet 14 would contain a Mn reversal along its profile. However, Garnet 14 has a core value of 8.9 wt.% MnO, higher than any value found in the profile of Garnet 10, which is impossible under the equilibrium scenario if Garnet 14 nucleated after Garnet 10. So both possible sequences of nucleation are inconsistent with a scenario in which Mn maintains rock-wide equilibrium throughout all stages of garnet growth.

The Mn reversals are therefore expressions of partial chemical disequilibrium (*cf.* Carlson 2002), and although their exact origin remains unclear, plausible explanations arise in the context of diffusion-limited growth and equilibration. *Partial* and *compound* crystals of garnet represent growth at locations where the supply of components needed for growth is restricted, either by local competition (*compound* crystals) or by adjacency to barren matrix (*partial* crystals). (The apparent "truncation" of partial crystals cannot represent shearing or dissolution of originally symmetrical crystals, because such effects are seen only for crystals with a low-Mn core.) If the Mn sources in the matrix are widely dispersed precursor phases, whereas other components are more uniformly distributed at short length-scales, then in areas of locally restricted supply, the requirement of long distances of transport for Mn, combined with its sluggish diffusion at low temperatures, could account for the low central contents of MnO in *partial* and *compound* crystals of garnet.

The outward increase in Mn may represent progressively larger scales for intergranular diffusion of Mn during prograde growth, as rates of intergranular diffusion increase exponentially with temperature. At the time represented by crystallization of the dominant Ca spike, rates of intergranular diffusion were apparently sufficiently rapid to achieve rock-wide chemical equilibrium for all major elements, insofar as all garnet crystals have equivalent concentrations there. It is likely that the maximum in the Mn-reversed profiles closely represents the point in time and temperature at which rock-wide equilibrium for Mn was achieved.

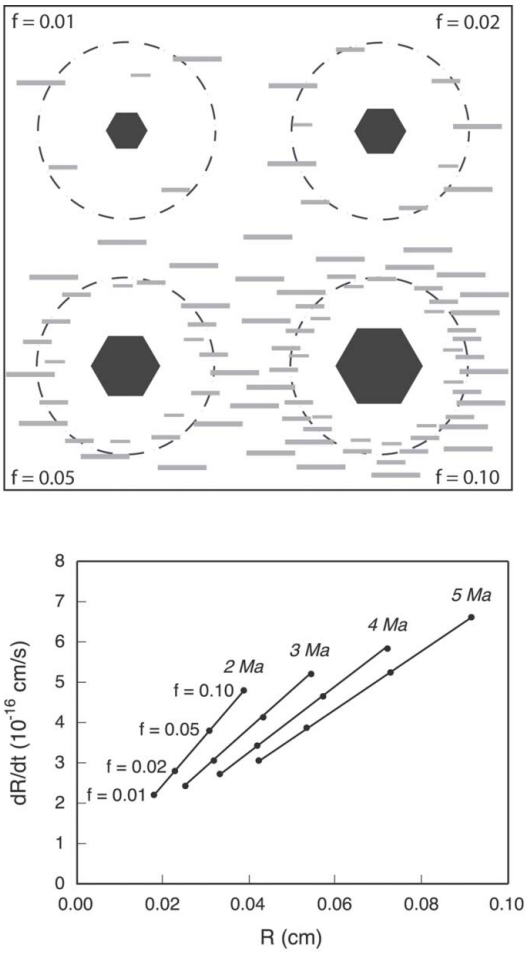

FIG. 12. (Top) Schematic illustration of diffusion-controlled growth of garnet from a heterogeneous precursor. Variations from one region to another in volume fraction *f* of aluminous precursor phases (*gray rectangles*) produce differences in growth rate and size of garnet porphyroblasts (*black hexagons*), because equivalently sized source-volumes for nutrients supplied by diffusion (*dashed circles*) yield different fluxes of nutrient in each region. (Bottom) Calculated growth-rates and radii for crystals in different regions at successive times, assuming simultaneous nucleation followed by thermally accelerated, diffusion-controlled growth obeying Equation [1] of the text.

Origin of Ca zoning patterns. Fine-scale Ca oscillations like those seen in the garnet of AG4 are rare in regional metamorphic rocks. Their origin in sample AG4 is unknown, but several possibilities deserving consideration are examined here.

The intricacy of Ca zoning patterns in sample AG4 is not likely to be the consequence of changes in pressure and temperature because nearby rocks of apparently similar composition, at several locations a few tens of meters up-section in the same sequence, do not contain similar patterns.

There is no evidence to suggest that the Ca oscillations represent changes in the garnet-forming reaction, because none of the other major cations show similar effects. Moreover, there is no detectable change in the mineralogy or abundance of inclusions in garnet throughout Zone 2, nor do these features differ between Zone 2 (oscillatory) and Zone 1 (not oscillatory).

Crawford (1977) demonstrated that garnet crystals growing from a mafic protolith in the Wissahickon Formation, Pennsylvania, had compositional variations that mimicked oscillations found in precursor plagioclase crystals. But plagioclase crystals in sample AG4, although zoned in Ca, do not show oscillatory zoning, nor do any of the other minerals for which X-ray maps were obtained.

Garnet grown in the presence of abundant hydrothermal fluids associated with igneous intrusions (such as skarn garnet from contact aureoles) commonly contains oscillatory Ca (*e.g.*, Jamtveit *et al.* 1995, Ivanova *et al.* 1998), but zoning in those crystals differs significantly from the zoning in AG4. In particular, oscillations caused by hydrothermal fluids typically cannot be correlated among garnet crystals on a hand-sample scale, unlike the Ca oscillations in garnet crystals from sample AG4. Furthermore, no intrusive bodies that might serve as sources for such fluids were introduced into the vicinity of Passo del Sole during garnet crystallization.

Stowell *et al*. (1996) found large oscillations in Ca in garnet from a contact aureole in southeastern Alaska. Noting that garnet further from the pluton had fewer oscillations than garnet closer to the pluton, they concluded that the oscillations were caused by episodic flows of Ca-bearing metamorphic fluid through the aureole, producing episodic growth of garnet. Although no intrusions are implicated, an otherwise similar scenario involving pulses of Ca-bearing fluids introduced into the Lucomagno nappe from the surrounding units might be invoked to explain the oscillatory character of Ca zoning in garnet from sample AG4. Sample AG4 was collected ~7 m from the contact of the Lucomagno nappe against a sequence of Triassic metasediments; these rocks at the contact are quartzose schists with small lenses of dolomite, but the metasediments a few

hundred meters distant are thick dolomites containing local evaporites (Chadwick 1968). Deformation could be linked to influx of fluids, because fluids decrease the yield strength of rocks, making them more susceptible to deformation, and because strain during deformation might produce local or transient dilations that would draw external fluids into the rock. In garnet crystals from AG4, the Ca oscillations begin shortly after the onset of deformation, as recorded by reorientation of the initially planar fabric included in the garnet crystals. Fluids might have introduced Ca scavenged from the carbonates or evaporites in numerous short pulses. Garnet growth in AG4 does not seem episodic, however, because the Ca changes do not correspond to changes in the Mn profiles, and spiral inclusion-trails show continuous changes in orientation. The absence of comparable Ca oscillations in garnet from nearby rocks requires that the postulated influxes of fluid were restricted to the stratum from which AG4 came. The presence of discontinuous layers of quartz in AG4, which may represent deformed and disrupted veins, contrasts with the absence of such features in nearby samples, lending some support to this hypothesis.

Origin of Fe and Mg zoning patterns. Patterns of Fe and Mg zoning tend to show features antithetical to those of both Mn and Ca, and their variations are likely to reflect compensation for changes in the local availability of Mn and Ca. As stated above, garnet crystals with low Mn at their nucleation sites have high central concentrations of Fe and Mg. Where the Ca zoning displays high spikes, Fe and Mg display correspondingly low bands.

Alternative mechanisms of crystallization

Interface-controlled growth. Brief consideration is sufficient to rule out the alternative of interfacial controls on the rates of garnet growth. Growth rates will be governed by interfacial attachment processes only if diffusion of species through the intergranular medium is rapid enough to eliminate gradients in the chemical affinity for reaction during the crystallization interval. The growth suppression seen in the MCF argues against this possibility, as it would not appear in an interface-controlled case, and the observed relationships between radii and zone widths are inconsistent with such a mechanism, which should instead yield size-independent rates of radial growth (*cf.* Kretz 1974, Carlson 1989).

Growth rates determined by advective transport. If the Ca oscillations in garnet are the result of open-system modifications of the composition of the intergranular fluid, as suggested above, then advective transport must have played some role in garnet crystallization, at least intermittently, and at least for some elements. One could even hypothesize that advective transport is the dominant factor governing the garnet nucleation-and-growth kinetics. In that case, the relationship between garnet sizes and growth rates in sample AG4 would reflect heterogeneity in advective fluxes of nutrients rather than heterogeneity in nutrient fluxes due to local abundance of the precursor; larger crystals would be produced along paths of advective flow for nutrient-rich fluids, whereas smaller crystals would be produced along paths of advective flow for nutrient-poor fluids.

A primary argument against advective-flow-related kinetic controls in sample AG4 is as follows: to govern the crystallization kinetics, the fluxes of components provided by advective flow must predominate over the fluxes generated by local breakdown of reactants. The nutrient fluxes reaching each growing crystal will be a combination of the material fluxes transported to the crystal surface advectively in the fluid and the material fluxes transported by diffusion from nearby precursors. Particularly in the case of intermittent, episodic infiltration of fluid, advective fluxes will predominate over local diffusional fluxes only for components that have low bulk-concentration locally in the precursor assemblage and that also have high concentration in the advecting fluid. The solubility of Al in metamorphic fluids is so low (*e.g.*, Walther & Woodland 1993, Walther 2001, 2002), and its local abundance in micaceous precursors is so high, that it is difficult to conceive of growth rates controlled by its advective supply: the amount of Al brought in by flowing fluids would be only a tiny fraction of the amounts locally available. In marked contrast, advective fluxes of Ca might well dominate over diffusive fluxes, given the low concentration of Ca in the bulk solid and its likely high solubility in chloride-bearing (and sulfate-bearing?) fluids (Popp & Frantz 1979).

Spatial relationships among garnet crystals also provide arguments against a significant role for advective transport as a rate-controlling mechanism. The observed correlation between crystal size and crystal isolation would not be predicted for the advective-flow case; in fact, just the opposite might be expected: large crystals should tend to be concentrated near one another along the paths of advective flow for nutrient-rich fluids. Furthermore, the observed near-neighbor size-isolation correlation is superimposed on a clustered distribution of garnet crystals, in which crystals of various sizes are interspersed at length scales of a few nearest-neighbor distances. That distribution is easily reconciled with patchy heterogeneity in precursor abundance, but would require a highly implausible complex intertwining of non-intersecting paths of advective flow.

Comparison with crystallization mechanisms in prior studies

Because precursor heterogeneity is a common feature in metamorphic rocks, it is reasonable to ask why the simple linear relationship between radius and radial rate of growth has not been uncovered in prior studies of crystallization kinetics. The answer probably has to

do with the fact that sizes and growth rates of garnet crystals are in general the result of interactions between nucleation kinetics and the complex kinetics of diffusional fluxes, which rise exponentially with temperature, depend on precursor heterogeneity in three dimensions, vary with the scale of matrix grains and the connectivity of grain edges, and are modified in intricate ways by near-neighbor competition. Only with extremely careful or serendipitous selection of samples is it possible to deconvolve the multiple interactions among these factors, to isolate the underlying mechanisms that their interplay commonly obscures. This may be made apparent by contrasting the microstructures and nucleation-and-growth histories of garnet at Passo del Sole (this study) with those of the Picuris Range (Carlson 1989, Denison *et al.* 1997).

The Picuris Range rocks studied by Carlson (1989) and Denison *et al.* (1997) are quite homogeneous. At the scale of a hand sample, most are unlayered micaceous quartzites in which the small and uniform grain-size of the matrix (generally tens of μm) preserves homogeneity down to submillimeter scales. As a result, precursor heterogeneity is not a factor, so variations in porphyroblast sizes are exclusively the result of nucleation-and-growth kinetics, reflecting differences in times of nucleation and in the degree of near-neighbor competition.

By contrast, a key feature of sample AG4 from Passo del Sole is that nucleation was nearly simultaneous for all garnet crystals. This bit of luck eliminated the otherwise predominant effects of size variations that arise from progressive nucleation throughout the crystallization interval, and from exponential acceleration of diffusion to varying degrees at different stages of each crystal's growth. Without those factors, variations in crystal sizes were determined primarily by the local environment. As a result, the effects of precursor heterogeneity became salient features, readily observed given the unusual Ca zoning to highlight the relationship between radius and growth rate.

The strong implication is that all of these factors can be expected to operate during metamorphic crystallization. Except in rare cases, however, unequivocal evidence for their operation may not survive the complex interactions that take place among them.

Implications for chemical equilibration during metamorphism

A principal finding of this study is that the kinetics of intergranular diffusion may govern nucleation and growth processes even in metamorphic rocks undergoing active deformation, providing further evidence of the fundamental significance of this process to metamorphic reactions and textures. Although prior examples of diffusion-controlled kinetics have been largely dominated by (yet not exclusively limited to) instances of near-static crystallization, the present result should make it clear that these are not anomalous situations.

The larger significance of this finding is its implication that limitations exist on chemical equilibration during metamorphism despite the effects of ongoing deformation. When reaction kinetics are diffusion-limited, gradients must exist in the chemical potential of one or more species, a violation of the common assumption of rock-wide equilibration for all elements throughout a rock's metamorphic history. Carlson (2002) reviewed evidence in metamorphic rocks for partial chemical disequilibrium (meaning rock-wide equilibration for some elements but not for others) and speculated upon a generalized progression of degrees of equilibration for different elements that results from the kinetic controls imposed by intergranular diffusion. The evidence suggested that even though Fe and Mg might equilibrate at the cm scale under lower-greenschist-facies conditions, Mn might not equilibrate at that scale until upper-greenschist-facies conditions were reached, Ca and some trivalent cations might not until the middle amphibolite facies, and some elements (like Y and the REE) might not even in the lower granulite facies. Patterns of garnet zoning in AG4 add corroborative and

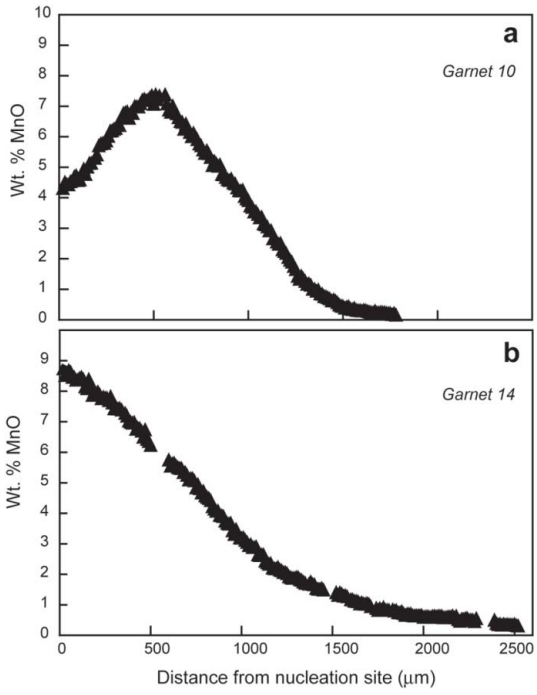

FIG. 13. Mn concentration along traverses from nucleation sites to outer rims for (a) partial Garnet 10 and (b) normal Garnet 14. As explained in the text, these relationships require disequilibrium for Mn during the early stages of garnet crystallization.

conflicting observations to these prior data on chemical equilibration during metamorphism.

On one hand, the unusual reversals in Mn zoning in cores of *partial* and *compound* crystals, interpreted above to result from restricted supply of Mn during initial growth, seem consistent with prior inferences regarding sluggish intergranular diffusion for Mn at low grade, as in the occurrences at Harpswell Neck, Maine, studied by Hirsch *et al*. (2003).

On the other hand, the complex oscillatory patterns of Ca zoning in garnet crystals from sample AG4 must reflect rock-wide equilibration for Ca under *P–T* conditions (~500–550°C, 5 kbar) very similar to those during garnet crystallization in the Picuris Range, New Mexico (~500–550°C, 4 kbar), in which Ca failed to equilibrate beyond mm-sized length-scales (Chernoff & Carlson 1997). As noted previously (Carlson 2002, p. 190), effective rates of intergranular diffusion depend on factors other than temperature. Any factor that affects the bulk solubility of elements in the intergranular medium is a potential control on their degrees of equilibration. A higher level of fluid saturation, greater abundance and connectivity of grain edges, and chemical factors such as higher chlorinity of the intergranular fluid are all possible, but still unconfirmed, explanations for increased length-scales of equilibration for Ca in the rocks at Passo del Sole compared to those in rocks of the Picuris Range. Alternatively, if the oscillatory Ca patterns at Passo del Sole are generated by the episodic influx of Ca-bearing fluids as suggested above, then perhaps the dissimilarity between the two occurrences is a record of the difference between Ca supply by advective flow in contrast to Ca supply by local diffusion. That hypothesis calls attention to a potential decoupling of reaction mechanisms between elements of high solubility whose equilibration could be governed by advective flow, and elements of low solubility whose equilibration would be governed principally by local availability.

Conclusions

Growth suppression among neighboring crystals, direct proportionality between garnet radii and radial rates of growth, and indications of early disequilibrium for Mn all constitute evidence that even during synkinematic crystallization, the kinetics of intergranular diffusion governed nucleation-and-growth mechanisms and the degree of chemical equilibration in the garnet gneiss of Passo del Sole. This result corroborates and enlarges upon earlier determinations that intergranular diffusion exerts a fundamental control on metamorphic reactions, extending that concept to the broad realm of rocks that undergo simultaneous deformation and metamorphism, and echoing insights that trace back to Dugald Carmichael's founding work some 35 years ago.

Acknowledgements

We thank John Rosenfeld (UCLA) for providing sample AG4, and for illuminating discussions of the textural implications of the crystallization kinetics of porphyroblasts. Wayne Dollase (UCLA) solved the tricky problem of correcting apparent widths to true widths of zones. Richard Ketcham performed the HRXCT scanning at the University of Texas High-Resolution X-ray Computed Tomography Facility. The software used to extract quantitative measurements from the HRXCT data was written by Richard Ketcham, with assistance from David Hirsch and Philip Watson; the software used to perform the calculations of correlation functions was written by David Hirsch. We gratefully acknowledge NSF grant EAR–9902682 for primary support for the work, the Geology Foundation of the University of Texas at Austin for ancillary support, NSF grant EAR–0004082 for support of the UT HRXCT facility, and NSF grant EAR–0113480 for support of HRXCT software development. Critical reviews by David Pattison, Tom Foster, and Chris Daniel produced valuable improvements in the final manuscript.

References

Adams, H.G., Cohen, L.H. & Rosenfeld, J.L. (1975): Solid-inclusion piezothermometry. II. Geometric basis, calibration for the association quartz–garnet, and application to some pelitic schists. *Am. Mineral.* **60**, 584-598.

Bell, T.H. (1985): Deformation partitioning and porphyroblast rotation in metamorphic rocks: a radical re-interpretation. *J. Metamorph. Geol.* **3**, 109-118.

_____ & Johnson, S.E. (1989): Porphyroblast inclusion trails: the key to orogenesis. *J. Metamorph. Geol.* **7**, 279-310.

Carlson, W.D. (1989): The significance of intergranular diffusion to the mechanisms and kinetics of porphyroblast crystallization. *Contrib. Mineral. Petrol.* **103**, 1-24.

_____ (2002): Scales of disequilibrium and rates of equilibration during metamorphism. *Am. Mineral.* **87**, 185-204.

_____ & Denison, C. (1992): Mechanisms of porphyroblast crystallization: results from high-resolution computed X-ray tomography. *Science* **257**, 1236-1238.

Carmichael, D.M. (1969): On the mechanism of prograde metamorphic reactions in quartz-bearing pelitic rocks. *Contrib. Mineral. Petrol.* **20**, 244-267.

Chadwick, B. (1968): Deformation and metamorphism in the Lukmanier region, central Switzerland. *Geol. Soc. Am., Bull.* **79**, 1123-1150.

Chernoff, C.B. & Carlson, W.D. (1997): Disequilibrium for Ca during growth of pelitic garnet. *J. Metamorph. Geol.* **15**, 421-438.

_____ & _____ (1999): Trace-element zoning as a record of chemical disequilibrium during garnet growth. *Geology* **27**, 555-558.

CRAWFORD, M.L. (1977): Calcium zoning in almandine garnet, Wissahickon Formation, Philadelphia, Pennsylvania. *Can. Mineral.* **15**, 243-249.

CROW, E.L., DAVIS, F.A. & MAXFIELD, M.W. (1960): *Statistics Manual*. Dover, New York, N.Y.

DANIEL, C.G. & SPEAR, F.S. (1999): The clustered nucleation and growth processes of garnet in regional metamorphic rocks from north-west Connecticut, USA. *J. Metamorph. Geol.* **17**, 503-520.

DENISON, C. & CARLSON, W.D. (1997): Three-dimensional quantitative textural analysis of metamorphic rocks using high-resolution computed X-ray tomography. II. Application to natural samples. *J. Metamorph. Geol.* **15**, 45-57.

_____, _____ & KETCHAM, R. (1997): Three-dimensional quantitative textural analysis of metamorphic rocks using high-resolution computed X-ray tomography. Methods and techniques. *J. Metamorph. Geol.* **15**, 29-44.

FISHER, G.W. (1978): Rate laws in metamorphism. *Geochim. Cosmochim. Acta* **42**, 1035-1050.

FOSTER, C.T., JR. (1986): Thermodynamic models of reactions involving garnet in a sillimanite/staurolite schist. *Mineral. Mag.* **50**, 427-429.

FOX, J.S. (1975): Three-dimensional isograds from the Lukmanier Pass, Switzerland, and their tectonic significance. *Geol. Mag.* **112**, 547-626.

FREY, M. (1978): Progressive low-grade metamorphism of a black shale formation, central Swiss Alps, with special reference to pyrophyllite and margarite bearing assemblages. *J. Petrol.* **19**, 95-135.

_____, BUCHER, K., FRANK, E. & MULLIS, J. (1980): Alpine metamorphism along the Geotraverse Basel–Chiasso – a review. *Eclogae Geol. Helv.* **73**, 527-546.

HIRSCH, D.M., KETCHAM, R.A. & CARLSON, W.D. (2000): An evaluation of spatial correlation functions in textural analysis of metamorphic rocks. *Geol. Mater. Res.* **2**, 1-41.

_____, PRIOR, D.J. & CARLSON, W.D. (2003): An overgrowth model to explain multiple, dispersed high-Mn regions in the cores of garnet porphyroblasts. *Am. Mineral.* **88**, 131-141.

IVANOVA, T.I., SHTUKENBERG, A.G., PUNIN, YU.O., FRANK-KAMENETSKAYA, O.V. & SOKOLOV, P.B. (1998): On the complex zonality in grandite garnets and implications. *Mineral. Mag.* **62**, 857-868.

JAMTVEIT, B., RAGNARSDOTTIR, K.V. & WOOD, B.J. (1995): On the origin of zoned grossular–andradite garnets in hydrothermal systems. *Eur. J. Mineral.* **7**, 1399-1410.

JOESTEN, R. (1977): Evolution of mineral assemblage zoning in diffusion metasomatism. *Geochim. Cosmochim. Acta* **41**, 649-670.

JOHNSON, C.D. & CARLSON, W.D. (1990): The origin of olivine–plagioclase coronas in metagabbros from the Adirondack Mountains, New York. *J. Metamorph. Geol.* **8**, 697-717.

KETCHAM, R.A. & CARLSON, W.D. (2001): Acquisition, optimization and interpretation of X-ray computed tomographic imagery: applications to the geosciences. *Comput. Geosci.* **27**, 381-400.

KILE, D.E. & EBERL, D.D. (1999): Crystal growth mechanisms in miarolitic cavities in the Lake George ring complex and vicinity, Colorado. *Am. Mineral.* **84**, 718-724.

_____ & _____ (2003): On the origin of size-dependent and size-independent crystal growth: influence of advection and diffusion. *Am. Mineral.* **88**, 1514-1521.

KRETZ, R. (1974): Some models for the rate of crystallization of garnet in metamorphic rocks. *Lithos* **7**, 123-131.

MAKOWITZ, A. & SIBLEY, D. (2001): Crystal growth mechanisms of quartz overgrowths in a Cambrian quartz arenite. *J. Sed. Res.* **71**, 809-816.

METH, C.E. (2002): *Diffusion-Controlled Growth from a Heterogeneous Precursor: Garnet Crystallization at Passo del Sole, Switzerland*. M.S. thesis, University of Texas at Austin, Austin, Texas.

MILNES, A.G. (1976): Strukturelle Probleme im Bereich der Schweizer Geotraverse – das Lukmanier-Massiv. *Schweiz. Mineral. Petrogr. Mitt.* **56**, 615-618.

NORDENG, S.H. & SIBLEY, D.F. (1996): A crystal growth rate equation for ancient dolomites: evidence for millimeter-scale flux-limited growth. *J. Sed. Res.* **66**, 477-481.

POPP, R.K. & FRANTZ, J.D. (1979): Mineral–solution equilibria. II. An experimental study of mineral solubilities and the thermodynamic properties of aqueous $CaCl_2$ in the system $CaO–SiO_2–H_2O–HCl$. *Geochim. Cosmochim. Acta* **43**, 1777-1790.

RAEBURN, S.P. (1996): *New Methods in Quantitative Metamorphic Petrology.* 1. *In Situ Determination of Iron Valence in Minerals.* 2. *The Application of 3-D Textural Analysis to the Study of Crystallization Kinetics*. Ph.D. dissertation, Pennsylvania State University, University Park, Pennsylvania.

RIDLEY, J. & THOMPSON, A.B. (1986) The role of mineral kinetics in the development of metamorphic microtextures. *In* Fluid–Rock Interactions During Metamorphism (J.V. Walther & B.J. Wood, eds.). Springer, New York, N.Y. (154-193).

ROSENFELD, J.L. (1970): Rotated garnets in metamorphic rocks. *Geol. Soc. Am., Spec. Pap.* **129**, 105.

_____ (1978): Snowball muscovite in the central Swiss Alps: an internal recorder of tectonometamorphism. *Geol. Soc. Am., Abstr. Programs* **10**, 481.

_____ (1987): Rotated garnets. *In* Encyclopedia of Structural Geology and Plate Tectonics (C.K. Seyfer, ed.). *Encyclopedia of Earth Sciences* **10**. Van Nostrand Reinhold, New York, N.Y. (702-708).

SCHONEVELD, C. (1977): A study of some typical inclusion patterns in strongly paracrystalline rotated garnets. *Tectonophysics* **39**, 453-471.

SPEAR, F.S. & DANIEL, C.G. (2001): Diffusion control of garnet growth, Harpswell Neck, Maine, USA. *J. Metamorph. Geol.* **19**, 179-195.

STOWELL, H.H., MENARD, T. & RIDGWAY, C.K. (1996): Ca-metasomatism and chemical zonation of garnet in contact-metamorphic aureoles, Juneau Gold Belt, southeastern Alaska. *Can. Mineral.* **34**, 1195-1209.

THAKUR, V.C. (1973): Events in Alpine deformation and metamorphism in the northern Pennine Zone and southern Gotthard Massif regions, Switzerland. *Geol. Rundsch.* **62**, 549-563.

WALTHER, J.V. (2001): Experimental determination and analysis of the solubility of corundum in 0.1 and 0.5 molal NaCl solutions between 400 and 600°C from 0.5 to 2.0 kbar. *Geochim. Cosmochim. Acta* **65**, 2843-2851.

_____ (2002): Experimental determination and analysis of the solubility of corundum in 0.1-molal $CaCl_2$ solutions between 400 and 600°C at 0.6 to 2.0 kbar. *Geochim. Cosmochim. Acta* **66**, 1621-1626.

_____ & WOODLAND, A.B. (1993): Experimental determination and interpretation of the solubility of the assemblage microcline, muscovite, and quartz in supercritical H_2O. *Geochim. Cosmochim. Acta* **57**, 2431-2437.

YANG, PANSEOK & RIVERS, T. (2001): Chromium and manganese zoning in pelitic garnet and kyanite: spiral, overprint, and oscillatory (?) zoning patterns and the role of growth rate. *J. Metamorph. Geol.* **19**, 455-474.

Received October 2, 2003, revised manuscript accepted July 15, 2004.

APPENDIX: KINETICS OF DIFFUSION-CONTROLLED GROWTH FROM A HETEROGENEOUS PRECURSOR

In this analysis, we seek to determine the relationship that should exist between zone widths and radii of porphyroblasts growing from a precursor with a heterogeneous distribution of the nutrient whose diffusion is rate-limiting for the crystals' growth.

Isothermal growth

Consider first isothermal growth under diffusion-controlled conditions of isolated spherical crystals, all of which nucleated simultaneously at time $t = 0$. The concentration of the critical element in the region of the matrix from which each crystal draws its nutrients is assumed to be locally uniform at the onset of crystallization, but concentration is assumed to be different from region to region.

This analysis ignores the complexities introduced by the buffering of nutrient concentrations by the reactant assemblage, and instead treats the region around each growing porphyroblast as a diffusional continuum. With that simplifying assumption, the radius of the spherical depleted zone from which each crystal draws its nutrients (R_{dpl}) is determined by the rate at which nutrients can diffuse through the intergranular medium (governed by the intergranular diffusivity D), and therefore is the same for all crystals at any chosen time t. On the basis of the characteristic diffusion-distance, the radius of the diffusionally depleted zone would be approximated as

$$R_{dpl} = (Dt)^{1/2} \quad [A1],$$

so the volume of the depleted zone (V_{dpl}) is given by

$$V_{dpl} = (4\pi/3)\, R_{dpl}^3 = (4\pi/3)\, (Dt)^{3/2} \quad [A2].$$

The volume of the crystal (V_{xtl}) inside any depleted zone depends upon the local bulk-composition, specifically upon the volume fraction f of the matrix that contributes to formation of the crystal:

$$V_{xtl} = f\, V_{dpl} = f\, (4\pi/3)\, (Dt)^{3/2} \quad [A3],$$

whence

$$R_{xtl} = f^{1/3}\, D^{1/2}\, t^{1/2} \quad [A4]$$

and

$$(dR_{xtl}/dt) = (\tfrac{1}{2})\, f^{1/3}\, D^{1/2}\, t^{-1/2} \quad [A5].$$

Crystals growing in nutrient-rich regions (large f) will have larger values of both R and dR/dt than crystals growing in nutrient-poor regions (small f). To determine how crystals grown from regions with different values of f array themselves in a diagram that shows R *versus* dR/dt for any chosen time, we examine the slope of the curve formed by this array of points, that is, the quantity d [dR/dt] / dR, in which both rate of radial growth and radius are functions of f. If this quantity is a constant, then a linear relationship exists between rate of radial growth (dR/dt) and radius R. To simplify the notation, we define two functions of f, one to represent radius and one to represent rate of radial growth:

$$x(f) \equiv R = [D^{1/2}\, t^{1/2}] \bullet f^{1/3} \qquad [A6]$$

$$y(f) \equiv \mathrm{d}R/\mathrm{d}t = [(\tfrac{1}{2})\, D^{1/2}\, t^{-1/2}] \bullet f^{1/3} \qquad [A7].$$

We seek the slope dy/dx for constant t, which is given by

$$\left.\frac{\mathrm{d}y}{\mathrm{d}x}\right|_t = \left.\frac{\mathrm{d}y/\mathrm{d}f}{\mathrm{d}x/\mathrm{d}f}\right|_t = \frac{(\frac{1}{2}D^{1/2}t^{-1/2})(\frac{1}{3}f^{-2/3})}{(D^{1/2}t^{1/2})(\frac{1}{3}f^{-2/3})} = \frac{1}{2t} \qquad [A8].$$

Because this quantity is a constant at fixed time t, there exists a linear relation between radial growth-rate ($y \equiv$ dR/dt) and radius ($x \equiv R$) on a diagram plotting these quantities at any chosen time for a number of different crystals, growing from regions with different concentrations of nutrients.

Prograde (*non-isothermal*) *growth*

The effect of variable temperature during the crystallization interval would be to cause the diffusion coefficient D to take on different values as a function of time, because it is an exponential function of temperature. This would of course have an important effect on the actual values of both the growth rate and the radius as functions of time, but the linear relationship between zone width and radius persists, because changes in the value of D in the numerator of Equation [A8] are offset by changes in the value of D in the denominator. This was confirmed by assigning an Arrhenius-style temperature dependence to the intergranular diffusion coefficient D, so that

$$D(T) = D_0\, exp\left(\frac{-Q}{RT}\right) \qquad [A9].$$

An exact analytical form of the derivative for the growth rate when Equations [A9] and [A10] are substituted into Equation [A7] was obtained from Mathematica®. In the main text, equations [A6] and [A7] are evaluated, using values from Carlson (2002) of $D_0 = 3.0 \times 10^{-11}$ m^2/s and $Q = 140$ kJ/mole, and assuming that prograde crystallization began at 500°C, with a heating rate of 10°C / Ma, so that

$$T = 773 + 10\, t \qquad [A10]$$

for t in units of 10^6 years. No departure from linearity on a rate *versus* radius diagram ($R^2 > 0.99999$) is revealed by those calculations.